Integrated Approaches for Understanding and Enhancing Natural Hydrogen Generation and CO_2 Sequestration in Geological Systems

By

JEFFREY KWASI AKUOKO

JUNE 2024

CHAPTER 1

1.0 INTRODUCTION

Due to its extensive use, energy has been the backbone of several if not all world economies. Till today, the major source of energy powering almost all technological endeavours is fossil fuel and its derivatives. The entity continues to feed the exponential advancements in technology, especially in transportation and industry. After its discovery in Titusville, Pennsylvania, fossil fuel has served its purpose very well in all departments of life, from powering homes to using drugs and clothes, among others. Though its merits have been well pronounced to date, the negative externalities associated with fossil fuels have and continue to have daunting effects, especially on climate and to some extent human life.

These effects have necessitated governing bodies and environmental groups to push the frontiers for finding new and cheaper alternatives to fossil energy and establishing frameworks to reduce and transition from fossil fuel use [1]. The criteria for these alternatives demand both cleanliness and affordability to ensure their widespread adoption and effectiveness in mitigating climate impact. To this end, though fossil fuel use cannot be completely exterminated, various alternatives and methods have been suggested to either replace oil and gas or serve as a strategy for limiting its effects. The latter involves carbon capture and storage, which involves both in situ and ex-situ methods [2]and has recently gained traction for being an effective method for contributing to net zero emissions. The former is the adoption of hydrogen which is seen from a scientific and chemical standpoint as a cleaner source in its comparison to fossil fuels.

Paradoxically, hydrogen being one of the most abundant chemicals is not easy to procure. The substance either exists as part of water with oxygen or exists deep in the earth [3]. Also, the dynamics involved and the workflow for hydrogen production are somewhat similar to the production of derivatives of fossil fuels when considering drilling for natural hydrogen, but the tools needed for its production remain quite underdeveloped[4]. Hydrogen is produced using varied methods, and its uses and prospects seem enticing as a fossil fuel replacement. Its uses span from the production of fertilizers to steel production. It could be used in powering industrial machinery as well as serve the purpose during chemical combination in a fusion reaction to produce helium. The latter, which is often explored as a twin chemical with

hydrogen [5] is often used in cooling superconducting magnets in MRI and could also serve as a shielding gas during welding [6]

The method employed for a specific hydrogen produced determines its nomenclature. For instance, hydrogen produced from reforming methane with steam is termed grey hydrogen. At present, most of the world's hydrogen is realised using this method. However, like fossil fuel refining, it emits greenhouse gases. In contrast, blue hydrogen captures and stores CO_2 emissions, offering a more environmentally friendly alternative [7]. Another variant is green hydrogen, produced from electrolysis where electricity is used in splitting water into its constituents (primarily hydrogen and oxygen). This water-splitting method has been adopted by various countries, as developed projects for green hydrogen continue to serve as supplements to these nations' existing energy mix. Another peculiar type, orange hydrogen has been highlighted by a few authors recently [8], [9]and the production process highlights a twin affair in sequestering CO_2 and producing hydrogen in a concomitant process.

Gold hydrogen, herein referred to as natural hydrogen, which has been delineated as the hydrogen of choice, is obtained from subsurface rocks and fits into the criteria of being relatively cheaper when compared to the types mentioned above. It is estimated that its production costs are in the region of $0.5 - 1 per kg against grey, blue, and green hydrogen with costs estimated at $0.9-3.2 per kg, $1.5-2.9 per kg, and $3.0-7.5 per kg respectively [10]. Also, apart from gold hydrogen whose demands are quite less exorbitant, all the others require a combination of processing facilities, a CCS facility, electricity, or a substantial amount of pumped water, and energy [11]

For natural hydrogen, though various discoveries continue to roll out, one which stands prominent is the discovery in Mali [12], [13], and has paved the way for research and exploration. Few authors have suggested that the accumulation of natural hydrogen has been underestimated, and also point out that the lack of attention it has received is due to the over-reliance on oil and gas. They argue that if deliberate efforts are made towards exploring natural hydrogen, the gas would be found in large accumulations[14], [15].

Various methods are used in producing hydrogen, as discussed earlier. However, natural hydrogen production follows distinct mechanisms dictated by specific geochemical reactions. These reactions include serpentinization, radiolysis, organic matter decomposition, and hydrogen occlusion. In serpentinization reactions, the interplay is between water's reaction

with iron-rich, mantle-derived ultramafic rocks which get hydrated to release hydrogen gas. For radiolysis, radioactive-rich rocks, mostly uranium-rich rocks in their interaction with water break the fluid into its constituents of hydrogen and oxygen, and with hydrogen occlusion, metals with a fixed and crystalline structure provide an avenue for trapping molecules in their interstitial sites. The release of hydrogen can then be attributed to fault zone cataclasis [16]. Natural hydrogen can also be produced by the anaerobic decay, fermentation, and nitrogen-fixing bacterial activities that break down organic matter. These processes frequently occur in complicated chemical and biological systems, where the hydrogen produced is subsequently taken up by microorganisms that consume hydrogen or transformed into nitrogenous chemicals and hydrogen-fixing methane by complementing reactions in soil and sediments [17]. Additionally, hydrogen generation through thermogenic processes of coal maturation has also been reported [18]

The recent conversation regarding energy transition and net zero emissions underscores the need for a continuous probe into the complex processes regulating natural hydrogen generation. Various research undertakings have laid solid foundations for understanding the natural hydrogen production process in the context of the major geological mechanisms. These works delve into adopting experiments to explain radiolytic reactions, hydrolysis for hydrogen production, serpentinization reactions, together with the secondary mineral assemblages formed after the metamorphosis of ultrabasic rocks, the partitioning of iron into secondary mineral assemblages, and hydrogen as a means for methane production through Fischer-Tropsch synthesis[19], [20], [21]. Despite these advances, several pressing issues require further attention, especially concerning the simultaneous process of natural hydrogen generation and CO_2 storage, the integration of catalysts to enhance natural hydrogen production from geologic reactions and the feasibility of other rock types in producing hydrogen.

CHAPTER 2

2.0 LITERATURE REVIEW

2.1 Hydrogen Production through Serpentinization

2.1.1 Introduction to Serpentinization

Ultramafic rocks are the most common sites of serpentinization. An ultramafic rock has fewer than 45 wt.% SiO2 and has high Mg and Fe concentrations. The origin and formation of ultramafic rocks on Earth are associated with crustal and volcanic processes. While the formation of ultramafic rocks differs across cosmic entities, their characteristics and classification remain consistent owing to their chemical composition and mineral makeup. These rocks can also be grouped based on the standardized ratios or prevalence of olivine and pyroxene minerals. Peridotites are ultramafic rocks with more than 40% olivine, while pyroxenites have less than 40% olivine[22].

Ultramafic rocks, though found in large quantities on Earth; are probably also found on virtually all solid celestial bodies in the solar system because olivine, the most prevalent silicate mineral, condensed during the solar system's initial formation [23], and their reaction with water is not only related to occurrences in the earth's interior but also space [22]. While considerable research has focused on the serpentinization process in terrestrial systems, there remains a dearth of literature regarding serpentinization in other planetary bodies that needs to be addressed.

When ultramafic rocks, which are rich in olivine and orthopyroxene, react with water, they become serpentinized, the resulting metamorphosed rock is composed primarily of serpentine. Serpentinite encompasses a broad category of ultramafic rocks that undergo serpentinization, a process where the degree of serpentinization and the presence of primary minerals in their residual form are not explicitly specified. H_2 is an important reaction by-product. The generic reaction can be used to sum up the process in general terms:

Olivine ± Orthopyroxene + H_2O → Serpentine ± Brucite + Magnetite + H_2. **(1)**

Frequently, reaction 1 is utilized to illustrate serpentinization reactions; however, it comes with a limitation in its representation that fails to fully encapsulate the intricacies of the chemical reactions occurring in natural settings. These portrayals excessively streamline the natural

processes, leading to an inflated estimation of the amount of H_2 generated in the reaction. In natural environments, a notable fraction of the released Fe (II) during serpentinization undergoes integration into solid solutions comprising serpentine and brucite, instead of magnetite. As a result, the Fe (II) incorporated into the serpentine and/or brucite solid solution remains inaccessible for oxidation to Fe (III) in magnetite, leading to a decrease in the quantity of generated H_2 [24]

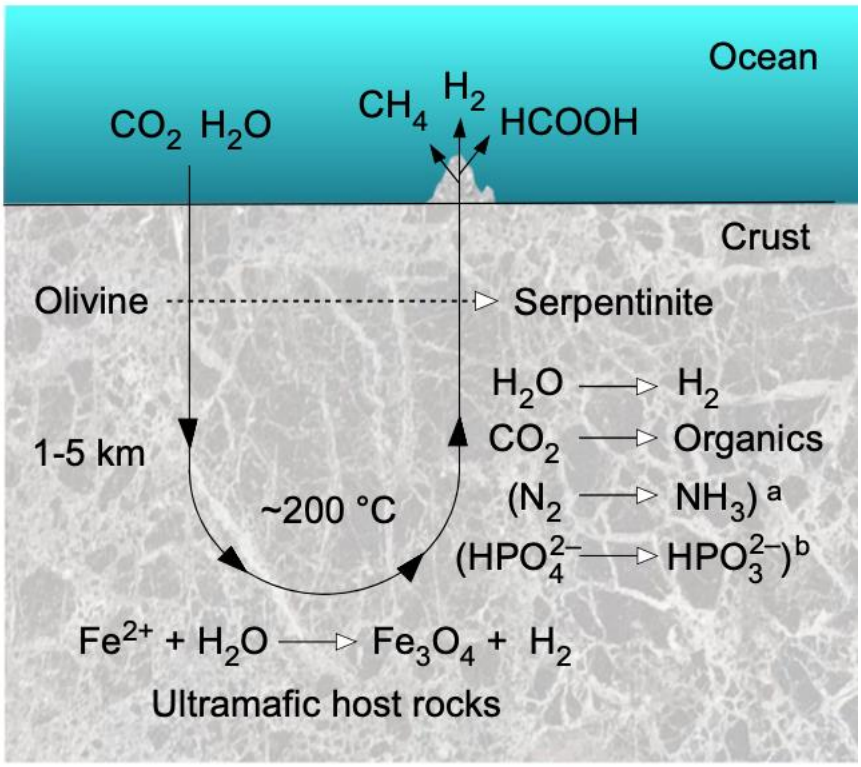

Figure 2.1. Apart from producing hydrogen, serpentinization can be viewed as a reducing agent. Surface water is pulled into crustal fissures during serpentinization, where it combines with ultramafic rocks at temperatures close to 200°C. Ferrous oxide in olivine is oxidised by water to Ferric oxide, which precipitates as magnetite throughout the reaction, producing H_2. Taken from[23]

2.1.2 Geological Conditions Favouring Serpentinization Reactions

Notable occurrences of serpentinization reactions have been attributed to mid-oceanic ridges in the sea floor, and ophiolite complexes on land, though there has been a proposition to explore cratonic basins [25]. In this model, it is suggested that, for exploration, geoscientists can fall on several major cues including but not limited to a protolith in Precambrian greenstone, the existence of groundwater, a fault that would serve as a conduit for transport and an overlying sediment that would serve as a reservoir. The formation of ophiolite complexes on land involves certain fascinating geological events of tectonics, obduction and accretionary processes.

Ultramafic Rocks (Peridotites): Ophiolites typically begin with the formation of ultramafic rocks, predominantly peridotites, originating from the upper mantle. These rocks are primarily composed of olivine and pyroxene minerals and are brought to the surface through processes such as magmatic intrusion or tectonic uplift.

Mafic Rocks (Gabbros): As oceanic spreading centres generate new crust, magma from the mantle solidifies beneath the ocean floor, forming mafic rocks, mainly gabbros. Gabbros are coarse-grained igneous rocks consisting mainly of plagioclase feldspar and pyroxene.

Basalts: Basaltic lava erupts onto the ocean floor at spreading centres, forming the uppermost layer of oceanic crust. Basalts are fine-grained igneous rocks composed primarily of plagioclase feldspar, pyroxene, and olivine. They overlay the gabbros and are the most abundant rock type in ophiolites.

Sedimentary Rocks: Sedimentary rocks accumulate along the margins of spreading centres through processes like erosion, deposition, and lithification. These sediments may include clay, sand, and carbonate materials. Through the process of obduction, ophiolites are transported from the oceanic realm to the continental realm, where they are preserved as slices of ancient oceanic crust and upper mantle [26]

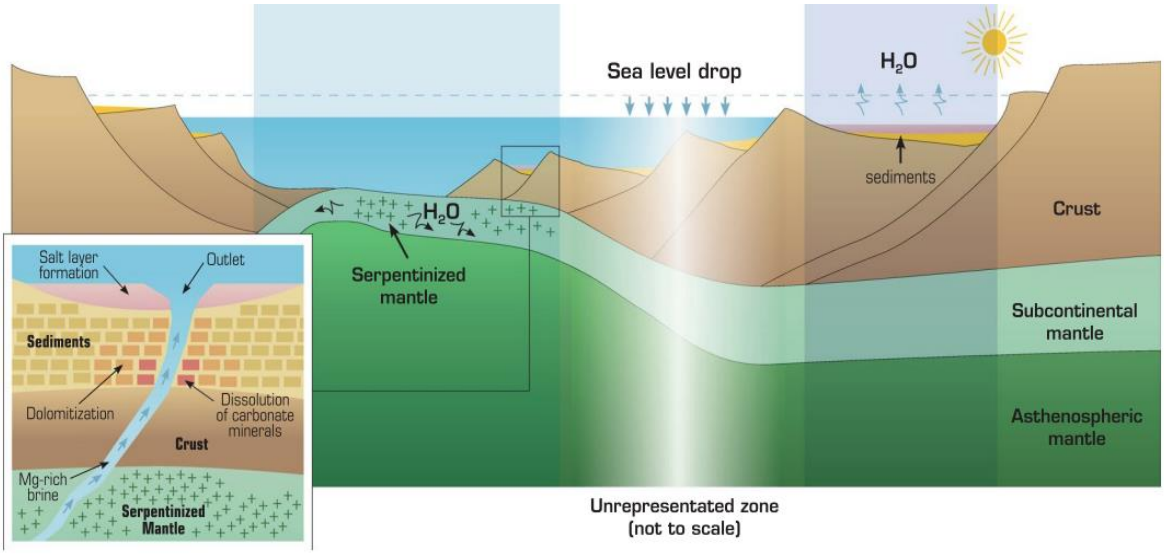

Figure 2.2 Typical serpentinization reactions include reactions between water and exposed mantle-derived rocks and between water that seeps through fissures during ridge spreading, and mantle rocks. [Insert]: The aftermath of serpentinization reactions can include the transport of hydrogen with the Mg-rich brine to the seafloor. Taken from [27]

Table 2.1 Possible Serpentinization Reactions Around the World

Country/Region	Geology	Possible reactions	H2 volume/Concentration	Temperature/ Flowrate	Reference(s)
Albania/Bulqizë	The mine is situated within the Bulqizë Jurassic ultramafic massif.This massif is a component of the giant Eastern Mediterranean supra- subduction-zone ophiolite belt	Serpentinisation (Could be properly ascertained if concrete info is gathered on the characteristics of reacting mine fluids Eg.pH)	Reported findings indicating a substantial outgassing rate of 84% (by volume) hydrogen (H2) from the deep underground Bulqizë chromite mine in Albania. At least 200 tons of hydrogen are released annually from the mine's tunnels.	A gas flow rate of 5±1L/s (at 25°C and 1.031×105 Pa)	[28]
Bosnia and Herzegovina	Dinaride ophiolite	Reaction of ophiolites with hyperalkaline groundwaters pH > 9 with possible spinel (chromite) catalysis	Mostly centered on CH4 concentrations ranging from 83 to 2706 mM (6e56 vol.% in the extracted gas-phase), but highest H2, 348.15 uM reported in the Vaiceva voda (Karanovac) site	Temperature (13-to-30-degree Celcius)	[29]
Oman	Oman ophiolite of Semail Nappe in the Northern Mountain of the Sultanate of Oman	Serpentinisation reactions between ophiolites and hyperalkaline warm springs	Highest hydrogen gas concentration of (377 µmol/l) recorded at Wadi site 28	Temperatures vary from 20.9 to 29.9°C	[30]

Country/Region	Geology	Possible reactions	H_2 volume/Concentration	Temperature/ Flowrate	Reference(s)
New Caledonia	Large outcrops of ophiolitic rocks (mainly peridotites)	fluid-rock interaction between ultramafic peridotite rocks and water of high alkalinity, pH > 10	H_2 between 26 and 36%	Temperature (23-to-40-degree Celsius) and flow rate of between 4 to 6 m3/day of gas	[31]
North Carolina (USA)	Carolina bays which are enigmatic geological features characterized by shallow, elliptical depressions or wetlands scattered across the landscape	Possible reactions producing H2 is unclear, but a complex and combinatory geological process could be involved	Large hydrogen volume of 3700 PPM based on field measurement recorded for the Jones Lake Bay	Flowrate of between 21–3060 m3/day/km2 for the three sites with average area of 2.62 km2	[32]
Liguria, Italy	Voltri Massif, which is part of the Penninic ophiolites	Serpentinization reactions between ophiolites and hyperalkaline warm springs	H_2(g) concentrations range from 0.011% (L43) to 1.2% (GOR34) of the total gas volume	Temperatures vary from 21.4 to 23.7°C	[30]
Philippines	Zambales Ophiolite	Serpentinization reactions with hyperalkaline fluids	CH_4 (55 mole%) and H_2 (42 mole%),	Temperature between 110–125°C	[33]

Country/Region	Geology	Possible reactions	H2 volume/Concentration	Temperature/ Flowrate	Reference(s)
USA, Kansas	Study areas are positioned near the Nemaha uplift just a short distance to the west of the Humboldt fault. This fault traverses both Precambrian basement rocks and lower Paleozoic strata.	Possible deep crustal iron oxidation of precambrian basement, with fluid pH < 8 and or hydrogen production from dissolved organic carbon	91.8% mole hydrogen gas for Sue Duroche#2 Well which reduced to about 0.1% mole in 2014	Temperature between 21 -22.6 °	[34]
Northern Oman	The Oman ophiolite, obducted onto the Hawasina Group of Permian-Cretaceous age, has been thrust over Late Permian to Late Cretaceous platform carbonates, initially deposited over the Precambrian basement of the Arabian Peninsula.	Serpentisation reactions	Hydrogen concentration ranging from 30 - 77% based on samples collected	Estimated flow rate between 73 - 147m3/km2 from peridotites and 340–1000 m3/km2 from overlying hawasina formation	[35]
Yanartas, Turkey	Tekirova ophiolite with harzburgite exposed at the surface, and consisting of brucite, hydromagnesite, serpentine, chrysolite, olivine, magnetite, lizardite, dunite, gers- dorfite, aragonite, and calcite	Serpentinisation with ultra-alkaline fluids characteristed by high pH of 11.95		Fluid temperature of 17.5 °C	[36]

Country/Region	Geology	Possible reactions	H2 volume/Concentration	Temperature/ Flowrate	Reference(s)
Moscow, Russia	Subcircular structures on igneous Precambrian rocks with overlying sedimentary cover	Reaction contributing to hydrogen generation not understood	Highest concentration of 8000 ppm recorded at Verevskoye		[37]
North California, US	The Cedars, located within Northern California's Coast Ranges, encompasses a segment of peridotite rock that accreted onto the continental crust as a component of the Franciscan Subduction Complex.	Reactions between Peridotites and ultra-alkaline pH between 11 and 12	Hydrogen concentration ranging from 15.7 - 51% between sites	Temperature of 17.2 ± 0.2 °C	[38]
New Caledonia	The New Caledonia Island group sits along the eastern edge of the Australian plate, near the western boundary of the Vanuatu subduction zone. A significant layer of oceanic lithosphere, which was thrust over continental basement during the late Eocene period.	Possible serpentinisation reactions between ophiolites and alkaline springs with pH ranging from 8 - 11	The gases released contain a volume of dry gas ranging from 12 to 30% hydrogen.	Temperature between 32 and 37 °C	[39]

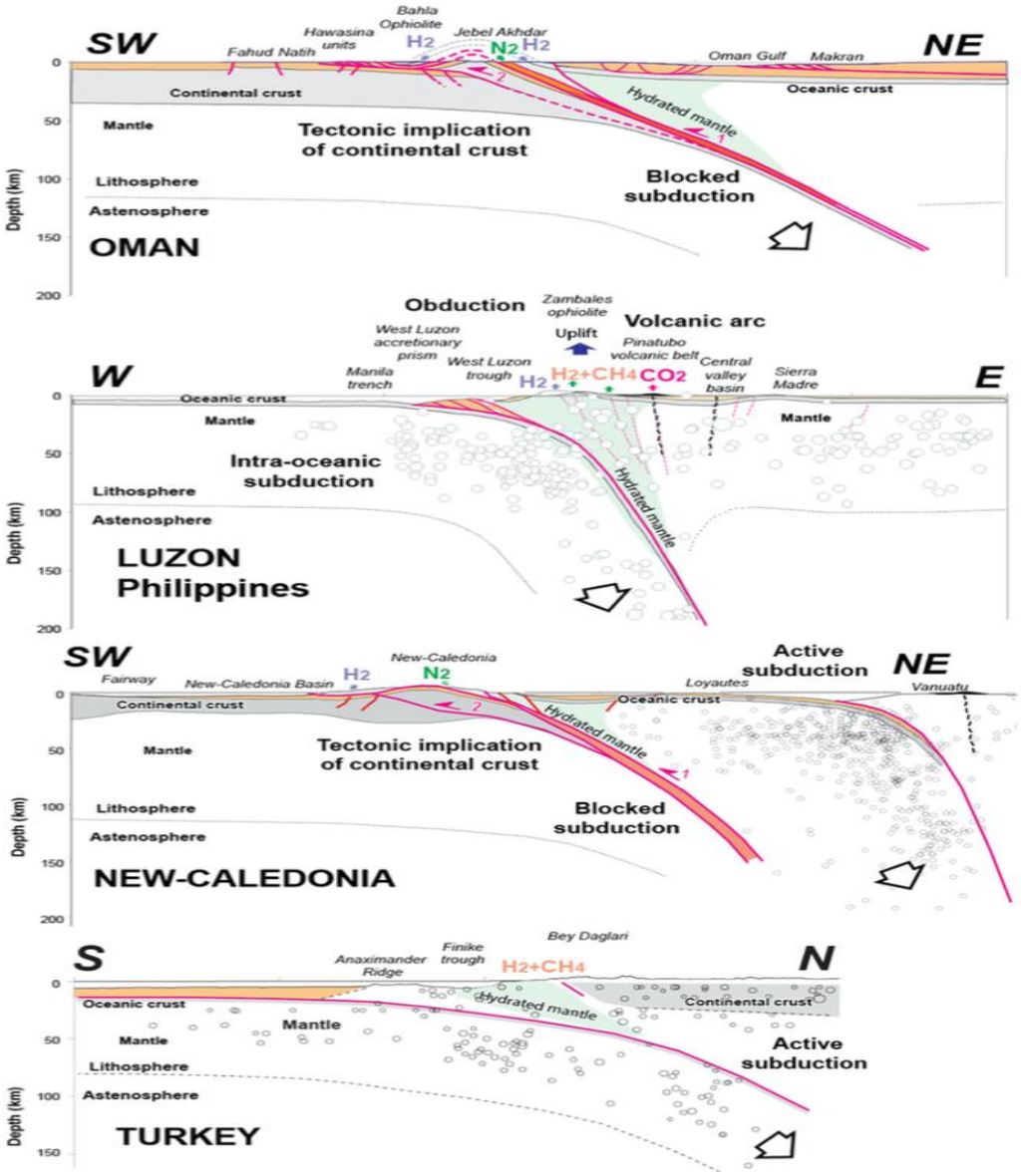

Figure 2.3 Serpentinization reactions involving ophiolite complexes in different areas. Oceanic materials (ophiolites) during tectonics get obducted onto the continental crust. Reactions are typical at tectonic margins where water seeps through cracks to react with both mantle rocks and obducted ophiolite complexes to produce hydrogen. Taken from [40]

Figure 2.4 Hydrogen seeps from a site in California. From supplementary material in [38]

2.1.3 Significance for Hydrogen Production

Living in a dispensation where sustainability is held in high regard, hydrogen production through serpentinization reactions can and will continue to be a major player in the quest for transitioning to cleaner energy. Though natural hydrogen exploration and exploitation have been quite recent, the geological process of natural hydrogen production through serpentinization has supported life for years. The hydrogen produced during serpentinization reactions on Earth has been a crucial element for biological communities. These organisms often inhabit hydrothermal vents, alkaline springs, and the subsurface and feed on the gas for their continuous survival [41]

For fossil fuel companies, one major consideration is the lifetime of the reservoir and the profits that can be accrued from exploiting non-renewable oil and gas. In sharp contrast, the geological processes that contribute to hydrogen production are an ongoing and unending process, which means, the gas can be produced continuously without the need to factor in the life of the reservoir during appraisals [42]. Though the need for hydrogen is indeed to curb and replace

fossil fuel-derived electricity and transportation fuel, there are minor contributing factors of hydrogen in producing various fluid species and organic compounds[22]. Apart from this, due to the diffusive nature of hydrogen, discovered reservoirs occupy large areas [13] and this could be expected for future discoveries especially if these discoveries are situated in cratonic basins. The size and accumulations can then compensate for the cost of production, and supplementary expenses.

2.2 Reaction Kinetics and Hydrogen Yield

2.2.1 Particle Size on Reaction Kinetics

For the serpentinization process, the stages for the complete reaction of the starting solid reactants and fluid to produce hydrogen are complex and less straightforward but can be quite concisely explained with the stages of reaction rate and consequently, the amount of hydrogen produced. Reaction rates of hydrogen have been studied in most experimental works, and the role of grain size of the reactants plays a key role. Small particle sizes in the region of about <30 μm, promote faster reaction kinetics in peridotites when compared to particle size in the region of about 100–177 μm in the same time scale. With these small particulate sizes, it is very likely to obtain almost complete serpentinization of the reactant in about 27 days of reaction [43]. The scenario and outcome of reaction rates for larger particulate sizes on reaction rates is less encouraging for pure olivine minerals when results show that just about 5.3% of reaction extent is achieved for sizes in the region of 100–177 μm for the same timescales. In general, pure olivine reaction rates prove to be very slow in comparison with peridotites, but reaction rates can be improved if smaller particle sizes are considered [44], [45]

In comparative terms, the justification for faster kinetics in larger particle sizes in peridotites as compared to pure olivine could be linked to the presence of spinel minerals which release Al and Cr in solution during serpentinization reaction processes. [43] proved this in experiments of mixtures of olivine and Al_2O_3 and Cr_2O_3 powders where the reaction extent improved tremendously. [46] also highlights the role of Aluminium in speeding up olivine dissolution and serpentine precipitation. Spinels are often constituents of peridotites in natural systems, and their contribution to reaction extent could be some inherent catalytic properties which tend to lower activation energies in serpentinization reaction processes [47]Though the enhancing properties of spinels in serpentinization processes have received some experimental backing, their functions can be limited by the pH of the reacting fluid, where acidic solutions tend to inhibit faster kinetics when compared to their alkaline counterparts[45]

2.2.2 Influence of pH on Reaction Kinetics

The influence of pH on reaction kinetics on various solid reactants has also received significant attention in the literature and contrasting views exist between authors. For acidic conditions, olivine minerals tend to exhibit certain fascinating dynamics. The reaction extent though temperature dependent is rapid in highly acidic conditions (2M HCl) but slower in neutral solutions [48], but exhibits a different dynamic by decreasing in CO_2-free solutions for increasing pH ranging from between 1 and 8 at a temperature of 25 degrees Celsius [49]. Alkaline solutions on reaction rates of olivine tend to agree somewhat with what is seen in highly acidic solutions, with increased reaction rates for hydroxyl solutions at higher pH [48], [50], though at lower temperatures the inverse occurrence is true [49]. These results, though temperature dependent have been proven for forsterites, and results to help understand the dynamics in the Fe-end member of Olivine (fayalite) are sparse.

For peridotites, which tend to be representative of most natural systems, their reaction in both acidic and alkaline solutions is distinct. Acidic solutions enhance their serpentinization rates, while highly acidic solutions decrease their rate. However, the extent to which reaction proceeds in hydroxyl solutions is unclear. While [48]highlights the negligible influence of alkaline solutions on peridotites, due to the consumption of hydroxyl ions by Al released in solution by pyroxenes causing neutral pH, [50] provides a different argument, and reveals that an increase in pH increases reaction extent in Olivine-pyroxene mixtures. The difference in results can be attributed to the presence of spinels in experiments conducted by [48] which also tends to release extra Al into solution causing the neutrality.

2.2.3 Influence of Salinity on Reaction Rates and Hydrogen Production

Serpentinization reactions are known to occur at mid-oceanic ridges [51] when seawater reacts with mantle-derived rocks from the oceanic crust and on fluid interaction with ophiolite complexes [52]**.** The characteristic fluid (seawater) which partakes in the reaction process is less likely to be pure and or anoxic, thus the presence of dissolved salts in serpentinization reactions cannot be ignored. The typical effects of salinity on olivine reaction rates in serpentinization processes need concise clarification to resolve the opposing findings that exist. [48], [53] asserts that high saline solutions enhance reaction rates in olivine, even greater, and double the percentage when compared to what can be observed for pure H_2O solutions (28%), increasing by about 62% in 7 days. It is important to note that water activity plays a key role in serpentinization reactions [54] and the presence of salts tends to reduce the activity of water

in partaking in serpentinization reactions thus reducing olivine dissolution rates [54][55] offers similar thoughts and agrees that the activity of water in serpentinization reactions is hindered by increased salinity, and the occurrence thus reduces the reaction extent of olivine. The experimental method adopted by [55] introduces such novelty in the manner in which salinity effects on olivine minerals are assessed, offering real-time examinations, and mimicking clearly how interactions can occur in nature.

In a contrasting scenario, [56] argues that NaCl enhances olivine dissolution rates due to the inhibition of a silica-rich surface layer on the olivine surface when performing experiments in assessing forsterite dissolution in saline water at an elevated temperature. While there have been two opposing views on the nature and effects of salinity on serpentinization extents in olivine, [57] introduces a different view, which highlights similar effects of both H_2O and saline solutions on olivine, this being in sharp contrast to what was established by [53]

Though the reaction kinetics of salinity on olivine have been assessed, works relating to the consequent effect on the amount of hydrogen produced are lacking. Here, reference would be made to the experimental work by [53] who reveals that saline solutions reduce hydrogen production in both olivine and peridotites when compared to reactions in pure H_2O from 123 mmol/kg in pure H_2O to 45 mmol/kg in a similar period for olivine. The decrease in peridotite hydrogen can be attributed to silica released from pyroxene during the hydrothermal reactions. Silica thus affects hydrogen generation in these processes[58]. These views on kinetics and hydrogen generation provide a platform for further research to help understand and address the existing empirical uncertainties.

2.2.4 The Role of Spinels in Hydrogen Production

Spinels are minerals that share a common crystal structure in the form AB_2X_4 and have a structure similar to the mineral $MgAl_2O_4$. The X are anions, which often exist as Se^{2-}, Te^{2-} or O^{2-} while the A and B are cations, A-site cations encompass various elements such as the alkali metal lithium (Li+), earth-alkaline metals like magnesium (Mg2+), calcium (Ca2+), and barium (Ba2+), as well as transition metals from the 3d series including manganese (Mn), iron (Fe), cobalt (Co), nickel (Ni), copper (Cu), zinc (Zn), alongside germanium (Ge), cadmium (Cd), and mercury (Hg). B-site cations are preferably constituted by aluminium (Al), scandium (Sc), titanium (Ti), chromium (Cr), manganese (Mn), iron (Fe), cobalt (Co), and nickel (Ni), in addition to gallium (Ga), indium (In), and thallium (Tl). These cations occupy the lattice structure. [59]

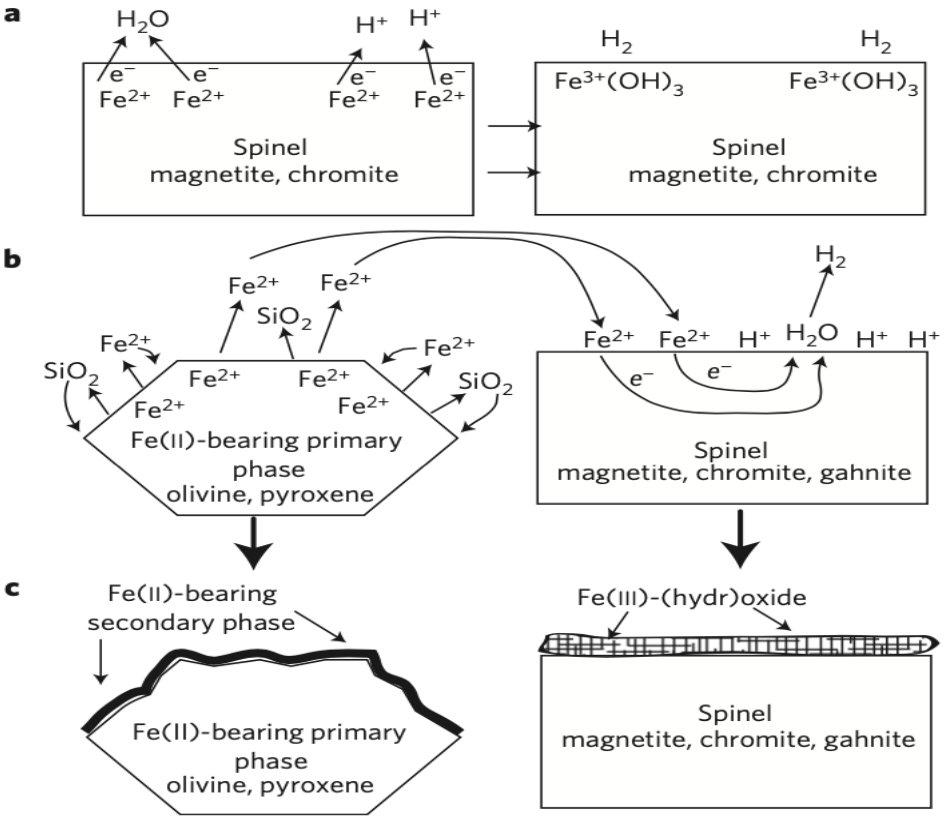

Figure 2.5. The role of spinel in hydrogen generation involves the process of; a) The spinel surface providing a platform for the adsorption of water molecules which then oxidizes structural Fe^{2+} in spinels to release H_2, b) Fe-bearing silicates releasing Fe^{2+} and SiO_2 in solution which gets adsorbed onto spinel surfaces where oxidation takes place with H_2O molecules to release hydrogen and c) The precipitation of secondary surface layers reduces the release of Fe2+ into solution which then affects H_2 generation in step (b). The adsorption of Fe (II) on the spinel surface also results in the formation of an oxidized surface layer, effectively protecting the spinel from further reactions. (c) (Right). Taken from [60]

The spinels' role in delivering faster kinetic rates also extends to hydrogen yield in serpentinization reactions. The mineral enhances hydrogen yield by around twice as much as solid reactants containing pyroxenes [61]. The inhibiting effect of pyroxenes on hydrogen yield is a result of the release of silica in solution which partakes in the serpentinization of olivine and thus incorporates into secondary minerals which precipitate in the serpentinization process [62]. The role of spinels in enhancing hydrogen is proposed to be attributed to the platform provided by spinels for the exchange of electrons from water to Ferrous oxides which initiates oxidation to ferric oxides on the surface of the spinels, thus enhancing the generation of hydrogen [60]. Even in the presence of CO_2-rich fluids, spinels still accelerate hydrogen production and work further in accelerating the reduction of CO_2 by up to three times than normal rates [47], [63]. One striking dynamic of spinels is their independent ability to produce hydrogen. The minerals have generally been considered catalysts to enhance hydrogen

production, but [64] highlights the possibility of magnetites in independently generating hydrogen.

2.2.5 P-T Conditions on Serpentinization Reactions

2.2.5.1 Temperature Effects

The ignition or spark necessary for serpentinization reactions is temperature. Temperature influences the reaction rate, equilibrium position, activation energy and reaction mechanisms in serpentinization reactions. Generally, the effects of temperature on the geological process of serpentinization reaction are limited by the stability of olivine at high temperatures [64], and for reactions involving the mineral, certain temperature ranges have been assessed together with their feasibility in generating hydrogen. Typically, hydrogen generation surges during a temperature range of between 200 and 300 degrees Celsius [44], but the stability of olivine at higher temperatures 400–500 °C introduces such sluggishness which reduces reaction rates and consequently hydrogen generation at higher temperatures [61]. These temperature ranges favour the crystallization of the mineral and make it more resistant to changes in temperature and pressure.

Though favourable conditions for serpentinization reactions have been established in the stated ranges of relatively high temperatures, several works have highlighted the possibility of the reaction at low-temperature ranges and the enormous production of hydrogen in these ranges [65][20][66]. The challenge that exists at lower temperatures is that, for natural rocks such as peridotites, and even olivine, the reaction process favours the evolution of the brucite secondary mineral assemblage, which incorporates in its structure the ferrous oxide Fe^{2+} that is needed for complete oxidation to the ferric state, for hydrogen production. [44] showed that the amount of Fe that partitions into brucite increases with decreasing temperature, while [66] corroborates this evidence with his finding on ophiolite serpentinization reactions. Results from [66]show that brucite formed at lower depths and relatively lower temperatures, which can in this context be seen as a reservoir of Fe^{2+} can still generate hydrogen that can support life at those depths. There has also been a contrasting finding on the negligible effects of temperature on hydrogen generation at temperatures in the region of about 30 to 70 degrees Celsius during olivine serpentinization reactions [65]. Though there is the possibility for such occurrence, in natural systems, where olivine does not exist in isolation but is often formed with spinels that can contribute to hydrogen generation, this finding still needs further assessment for concrete evaluation.

2.2.5.2 Pressure Effects

Pressure regulates both reaction rates and hydrogen production during serpentinization. Pressure effects on reaction rates of ultramafic rock serpentinization has received some considerable attention, however it is yet to be widely assessed how pressure impacts hydrogen production, especially for olivine. Pressure is a variable that contributes to hydrogen, and abiotic methane formation [67]

In these serpentinization reactions, confinement effects resulting from high pressure are very crucial since they influence the reactant-product distribution in the rock matrix and thus influence the reaction pathway. Pressure can also affect the solubility and activity of water during serpentinization reactions. Though water activity during high-temperature conditions has been assessed by [55], a gap for pressure effects still exists. Pressure effects cannot be overlooked when considering the thermodynamics of serpentinization reactions especially when the reaction phenomena depends on fluid flow, availability, and residence time with ultramafic rocks. Few studies have highlighted the effects of pressure on especially pure olivine reaction rates but the views on peridotites highlight the importance of the thermodynamic variable in serpentinization reactions.

Though these effects are not clear, it does one thing in revealing the essential role of pressure. Results from [62] show that reaction rates at lower pressure tend to be lethargic before increasing, and as pressure increases peridotite reaction extents increase proving this in their experiment conducted at 500 degrees Celsius for a pressure range of 3 and 20 kbar when their experiments show a 19% reaction extent at 3kbar for 20 days, rising to 96% reaction extent at 20kbar for the same time range. [68] presents opposing findings and argues that lower pressures rather contribute to accelerating serpentinization reactions while emphasizing the role of spinels in contributing to faster kinetics in olivine and the inhibition of orthopyroxenes in the process and continues to argue that peridotite serpentinization rate decreases with increasing pressure up to at least 35 Mpa at 230 degrees Celsius. Though these opposing views can be attributed to temperature differences under which these experiments were conducted, it is still important to verify these findings for a wide temperature range to address these concerns.

Pressure also affects the secondary mineral assemblages formed during serpentinization reactions. It is a controlling factor in how and what products can be formed during serpentinization reactions. Varying pressure can produce varying products from sib-green-shist at 4kbar to eclogite facies at 20 kbar in subduction zones [69] and even in experiments where

spinel effects are considered on peridotites serpentinization, varying pressure affects the serpentine mineral produced, from Lizardite and Aluminium lizardite to antigorite at a pressure of 1.8 Gpa [68]

2.3 Hydrogen Generation from Hydrolysis Reactions

Iron-containing rocks have shown promise in contributing to the production of natural hydrogen. Recent studies have proven the important role these rocks play in generating hydrogen. For example, current natural hydrogen generation occurrences have been attributed to Banded Iron Formations [70], [71], and the chemistry leading to hydrogen formation in these rocks is the generic Iron oxidation-hydrogen reduction process. Though the chemical drivers behind the hydrogen generation process for these rocks have been sparsely constrained experimentally, their association with recent discoveries prove their importance. BIFs do possibly contain greater iron content than their ultramafic counterparts, and it is quite astonishing the limited attention they have received regarding their experimental and theoretical assessment for hydrogen production.

Banded iron formation, known as BIF, is a sedimentary rock rich in iron, occurring in distinct layers or bands. The formation of BIF is influenced by the presence of ferrous iron and oxygen levels in seawater[72]**.** The rocks not only contain extensive data about the condition and development of the lithosphere and atmosphere but also harbour the largest portion of the world's valuable iron resources. Iron-rich sedimentary layers have been periodically laid down throughout Earth's history, yet it is the Precambrian epoch that hosts the most significant reserves of banded iron formations, characterized by layers of chert. Existing evidence, though not definitive, hints at three distinct periods of heightened deposition: the mid-Archean era (approximately 3400-2900 million years ago), the early Proterozoic period (approximately 2500-1900 million years ago), and the late Proterozoic epoch (approximately 750-500 million years ago). Notably, the deposits from the early Proterozoic era substantially surpass those from other epochs, collectively constituting more than 90 percent of the estimated total of originally deposited iron formations, amounting to approximately 10^15 tons [73]

Earlier investigations indicate that the iron found within Banded Iron Formations (BIFs) primarily originates from both hydrothermal fluid and continental weathering [74], [75]. The constituent of Banded Iron Formation could have originated from different sources. For instance, hematite arises from the dehydration of Fe(OH)3 during initial diagenesis, while. the genesis of magnetite is notably intricate and might occur throughout diagenesis, and

metasomatism processes. Also, siderite's source could be early inorganic precipitation, or it may have arisen from microbial transformative iron reduction processes [76] These processes illustrate the complex nature of BIFs and their importance in shaping the history and current state of the earth.

Though the lack of studies on BIFs is regrettable, the potential of basalts has been assessed. The findings from different studies on hydrogen production from basalt-groundwater interactions and microbial ecosystems present a comprehensive picture. Initially, it was concluded that hydrogen production is not feasible at environmentally relevant alkaline pH levels, with only transient production observed at lower pH in laboratory settings. Geochemical considerations suggested that these production rates could not be sustained over long geological periods, indicating that such interactions were unlikely to support microbial metabolism in the subsurface [77]. However, other research identified ferrous silicate minerals as crucial for hydrogen production in anaerobic water-rock interactions, noting that hydrogen evolution was faster at pH levels below 7 but still occurred between pH 5 and 11, encompassing the natural pH range of CRB groundwaters (7-10). This study found that hydrogen production coincided with the presence of dissolved Fe^{2+}, and the apparent alkaline inhibition could be alleviated by adding excess $FeCl_2$. Moreover, higher temperatures (e.g., 60°C) significantly increased hydrogen production rates compared to lower temperatures (e.g., 30°C), suggesting that geothermal gradients could enhance hydrogen production at greater depths [78]

Bacterial communities have been detected in deep crystalline rock aquifers within the Columbia River Basalt Group (CRB). CRB groundwaters contained up to 60 pM dissolved hydrogen, and autotrophic microorganisms outnumbered heterotrophs. Stable carbon isotope measurements implied that autotrophic methanogenesis dominated this ecosystem and was coupled to the depletion of dissolved inorganic carbon. Laboratory experiments demonstrated that hydrogen, a potential energy source for bacteria, was produced by reactions between crushed basalt and anaerobic water. Microcosms containing only crushed basalt and groundwater supported microbial growth. These results suggest that the CRB contains a lithoautotrophic microbial ecosystem that is independent of photosynthetic primary production [79]While the earlier study emphasized the limitations in hydrogen production under typical environmental conditions and over long timescales, the recent findings highlight specific conditions (appropriate pH, presence of ferrous silicate minerals, and higher temperatures) that could indeed facilitate hydrogen production. Thus, while hydrogen production from basalt-

groundwater interactions may not be universally sustainable, under certain geochemical and thermal conditions, it could potentially support microbial ecosystems in the deep subsurface, particularly in the CRB where a litho-autotrophic microbial ecosystem has been identified.

The generic reaction of iron hydrolysis has controlled almost all reactions for hydrogen generation, however contributing factors of silica hydrolysis are also possible. Even at very low temperatures of about 0 degrees Celsius, silicate rock types of gneiss, quartzite, shale, granite, nepheline syenite, and schist have been shown to produce hydrogen [80]. For quartz, the active site generated by mechanical effects (fracture and attrition) also contributes to the chemical reaction that facilitates hydrogen production [81]. The formation of hydrogen through silicate rocks can be highlighted by the simplified free radical equation;

$$Si\bullet + H2O = SiOH + H\bullet \quad (2)$$

$$H\bullet + H\bullet = H2 \quad (3)$$

Quartz's reaction with water results in a trend of decreased pH because the water molecules break apart the silicon-oxygen bonds present in the quartz structure, resulting in the formation of silicic acid (also known as orthosilicic acid or H4SiO4) and the release of hydroxide ions (OH-). Silicic acid is a weak acid, meaning it partially dissociates in water to release protons. This leads to an increase in the concentration of H+ ions in the solution, thereby decreasing the pH. The formation of silicic acid and the subsequent release of H+ ions contribute to the acidity of the solution, leading to a decrease in pH. Quite surprisingly, these reactions have been shown to occur in nature, as there has been a discovery of hydrogen from Silica melt intrusion from Quartz in the Chinese Jiajika granite [82] and in France where significant hydrogen is generated from biotite-rich granites [83].

2.4 Hydrogen Generation from Radiolytic Reactions

Water radiolysis involves the breakdown of water molecules due to exposure to ionizing radiation, which generally comes from the decay of radioactive elements. The process happens in several quick steps. First, energy hits the water within a femtosecond, creating ionized and excited water molecules and free electrons. Next, these molecules undergo various fast reactions and changes in the following picoseconds. Finally, within microseconds, the resulting particles spread out and react with each other and nearby molecules, with recombination becoming less significant after about one microsecond for low-LET radiation [84]. The main

products of water radiolysis consist of various chemical species: eg, HO·, H·, HO2·, H3O+, OH-, H2O2, and H2 [85]. In the context of rocks, any rock that water has infiltrated would subject the water to α, β, and γ radiation due to the decay of long-lived radionuclides. When a section of the rock sample comes into contact with water, radiolysis guarantees continuous H_2 production in that area [86].

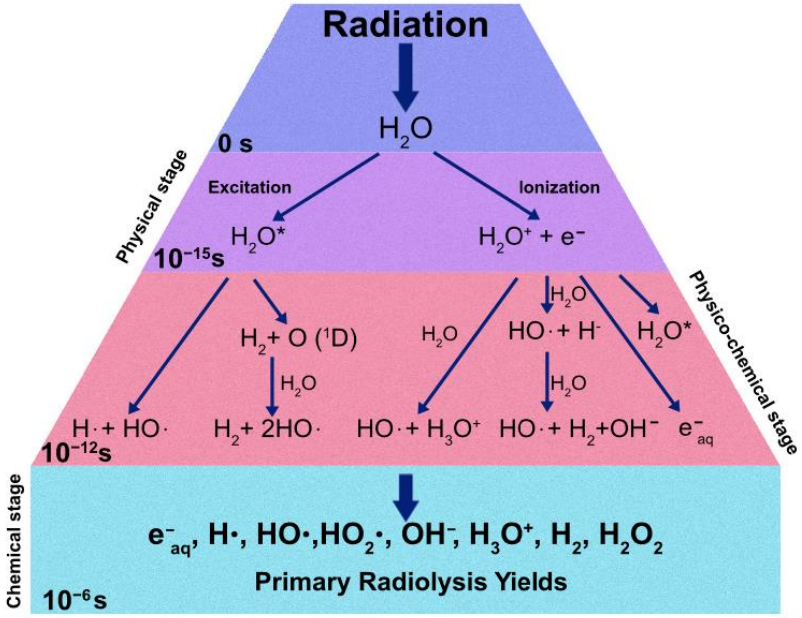

Figure 2.6 Stages of radiolysis reactions highlighting the primary products formed. Taken from [87]

Unlike serpentinization reactions, hydrogen generated via radiolysis is a self-sustaining process unaffected by temperature[88]. In geological contexts, radiolysis of rocks and subsequent hydrogen production can have various implications. For example, hydrogen generated through radiolysis may serve as a potential energy source for subsurface microbial communities in environments such as deep-sea hydrothermal vents or continental subsurface aquifers [16]. In geology, the radiolysis of water involves naturally occurring radioactive elements such as uranium (U), thorium (Th), potassium-40 (K-40), and radon (Rn) found in rocks and minerals. These elements undergo radioactive decay, emitting alpha particles, beta particles, and gamma rays, which can trigger the breakdown of water molecules and generate reactive species, influencing geochemical reactions in the surrounding environment. The radioactive isotope potassium-40 (40-K), which has a half-life of 1250 million years, undergoes decay primarily by emitting beta rays (89%) and gamma rays (11%), with an average energy of 0.455 MeV. The relative isotopic abundances of 40-K on present-day Earth and 4500 million years ago are 0.0117% and 0.145%, respectively [88] . The evidence of hydrogen production from radiolytic reactions can be supported by the fact that hydrogen gas produced in the subsurface is

instrumental in supporting microbial life. In specific underground environments, naturally existing hydrogen (H2) serves as a source of electrons for anaerobic microorganisms such as methanogens, acetogens, and sulfate-reducers, contributing to what is known as the "deep biosphere." These environments encompass volcanic and siliciclastic aquifers and marine sediments low in organic matter [89]. Understanding the processes involved in radiolysis can provide insights into the geochemical cycling of elements and the formation of secondary minerals in rocks exposed to ionizing radiation over geological timescales.

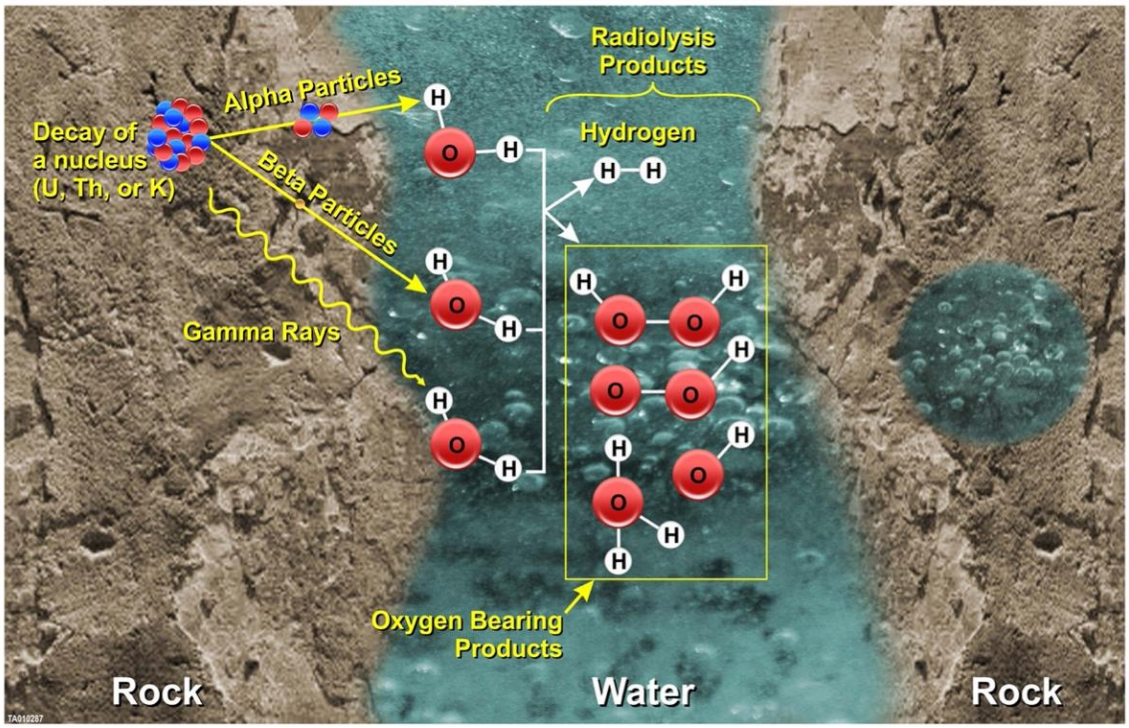

Figure 2.7 Water radiolysis as a result of radioactive rock-water reactions. The products of water radiolysis occur due to various physical and chemical processes that occur after water is excited or ionized by radiation. Taken from [86]

2.4.1 Modelling Radiolytic Reactions

It is important to understand the factors controlling radiolytic reactions as this helps optimize the conditions (such as radiation dose rate, temperature, and pressure) that can maximize hydrogen production efficiency. This optimization is crucial for making radiolysis-based hydrogen production economically viable and competitive with other methods. It also allows for predicting the yield of hydrogen and other byproducts formed during the process. Understanding the composition of these byproducts is essential for assessing the purity of the produced hydrogen and minimizing the formation of unwanted substances. In modelling

radiolytic reactions, it is important to understand how energy travels through water during the breakdown process.

To highlight this process [85]developed a model which measures how quickly water breaks down near radioactive solids and explains that the effect of energy on the breakdown is a function of the radiation type. For clarity, alpha radiation predominantly causes water breakdown near the surface of old spent fuel (1000 years old) with damaged cladding. Also, [90] split nuclear fuel and the water around it into layers to calculate how much radiation each layer gets using information about more than 200 types of radioactive material for their model and highlights that radiation from beta particles near the fuel's surface doesn't affect much. These models reveal the dynamics of radiation reactions but have mostly focused on nuclear fuels and less on the geological context.

2.4.2 The Influence of Porosity and Permeability on Radiolytic Reactions.

The efficiency of radiolysis depends significantly on the porosity and permeability of the rock formation. Porosity, which refers to the volume of empty spaces (pores) within the rock, is crucial in determining the amount of water available for interaction with radioactive materials. Higher porosity allows for greater water retention and exposure to irradiating substances, thereby influencing the rate of radiolysis, and the opposite is true for low porosity. For instance, low-porosity rocks (0.3 and 2.2%) in the Witwatersrand Basin, South Africa show little to no hydrogen [91]. Permeability, conversely, defines the rock formation's ability to transmit fluids through its pores. A highly permeable formation facilitates the movement of water, potentially enhancing the transport of radiolytic products and promoting more extensive chemical reactions. Conversely, low permeability restricts fluid flow, limiting the dispersion of radiolysis-induced substances.

Increased porosity, though improbable across an entire core body, can elevate radiolytic production by nearly tenfold, particularly in regions situated beneath the ocean floor [86]. Porosity and its influence on radiolytic reactions can also be analysed by comparison between occurrences on Earth and Mars. In places on Mars where the sediment is less porous (less than 35% space) and has small particles, the hydrogen production rates are mostly higher than in certain parts of Earth's ocean floor.

In areas with higher sediment porosity and cracked hard rock on Mars, the hydrogen production rates are similar to those in certain parts of Earth's ocean floor. However, in larger cracks on Mars, the hydrogen production rates are much lower [92]. Though this provides some insights into an external planet, these findings are based on models and need experimentation for validation. The decomposition of ancient fault rocks, plentiful in Mars' fractured crust, might also play a role in releasing H2 [93]. On earth, cracks and fracture processes may contribute to the release of H2 from various sources. Cataclasites, which are rocks formed by relatively mild seismic friction, exhibit lower and less uniform increases in hydrogen content. The detected increases in H2 levels correspond with the findings of laboratory experiments on H2 generation during rock fracturing performed by [93]

It is also possible for hydrogen to be produced at the nanoscale. When water is confined within the structure of zeolites 4A, there is a higher yield of hydrogen produced through radiolysis compared to when water is not confined within the zeolite structure, also, water molecules located specifically within the β cages of the zeolite structure are particularly effective at generating hydrogen through the process of radiolysis induced by gamma radiation [94]. Hydrogen is a key component of radiolytic processes and is crucial in various geochemical and biological processes. Porosity and permeability affect the rate and extent of hydrogen production, which can impact the chemical composition of subsurface environments and potentially support microbial life.

2.5 Enhancing Geochemical Reactions for Hydrogen Production

Most geochemical reactions that dictate hydrogen production are slow, taking significant timescales for considerable amounts of hydrogen to be generated. To simulate these mechanisms, lab experiments have mimicked the processes for long periods, especially for serpentinization reactions [20][44][50][95][96]. As the demand for clean energy increases, it is worthwhile to find ways to accelerate these geochemical reactions for faster hydrogen generation, and catalytic reactions can be very useful in solving the timescale problem. Catalysts are substances that speed up chemical reactions by lowering activation energy without being consumed. Technically, it facilitates the redistribution or relocation of atoms or electrons within the bound reactants from one site to another, resulting in accelerated product formation [97]. They are crucial in natural and industrial processes due to their efficiency and control over reaction dynamics. They come in various types such as homogeneous (same phase as reactants), heterogeneous (different phase, e.g., solid in gas), biocatalysts (enzymes), and

nanocatalysts (nano-sized particles) [97]. Catalysts work through mechanisms like adsorption (reactants adhere to catalyst surfaces) [60], intermediate formation (temporary compounds with reactants), and reducing activation energy (providing an easier reaction pathway) [98]. They are extensively used in chemical manufacturing, petroleum refining, environmental protection, pharmaceuticals, and clean energy production (e.g., hydrogen generation, fuel cells).

Catalytic reactions have been studied pervasively in the context of hydrogen production from crude oil-saturated rocks [99], [100], [101], [102], [103], but their efficiency in accelerating low-temperature reactions of serpentinization, and radiolysis for hydrogen production remains largely underexplored. Catalysts are efficient in accelerating Fischer-Tropsch synthesis processes. Most of these FTT processes typically occur in chromitites [104]. Chromitites are often found in association with ruthenium and at low temperatures of about 20 to 35 degrees Celsius, ruthenium proves useful in catalysing FTT reactions [105]Ruthenium has also been used in hydrogen production from ammonia decomposition, but the downside is its exorbitant price [106]. Nickel, chromium, cobalt, and nickel-based alloys can be viable options in terms of cost and efficiency. These metals are seen as less suitable for FTT synthesis because they support the process at high temperatures, where methane cannot be produced (> 150–200 °C) [105]. In contrast, the high-temperature range is conducive for serpentinization reactions and can be the right platform for these metals to accelerate serpentinization for hydrogen production.

A typical nickel-based alloy is awaruite. It is relatively stable under the conditions typically encountered in serpentinization reactions, such as elevated temperatures and pressures [107]. This stability ensures that the catalyst remains active over extended reaction times, contributing to its effectiveness in promoting the desired transformations. Awaruite's surface structure can facilitate the adsorption and activation of reactant molecules involved in serpentinization reactions. This can enhance the rate of reaction by providing active sites for the chemical transformations to occur. While the surface reactivity of the alloy provides the platform for catalysis, there is the likelihood for awaruite to passivate under highly alkaline conditions and at high temperatures [108]. In terms of abundance, it is often found in association with serpentine minerals in certain geological settings. Its abundance in these environments makes it a readily available catalyst for serpentinization reactions, potentially influencing the geochemical processes occurring within serpentinized ultramafic rocks [109]In radiolysis reactions, zirconia and ceria are typical catalysts that accelerate radiolytic reactions. Higher

yields of H2 were observed for one to two water layers on CeO2 and ZrO2 compared to bulk liquid water. The amounts of H_2 produced are noticeably influenced by the quantity of water absorbed unto the oxide particles. ZrO2 radiolysis generated approximately five times the amount of H2 compared to CeO2 when the same quantity of water was adsorbed [110]. Apart from these oxides, marine sediments (abyssal clay, clay-rich siliceous ooze, calcareous ooze, nannofossil-bearing clay (calcareous marl), and lithogenous sediment) are also capable of significantly enhancing yields compared to pure water, up to 27 times higher [111] If analogous catalytic materials on other planets contain water, the process of water radiolysis could potentially support life in those environments as well [111]

2.6 Introduction to Coupled Processes of H2 Production and CO2 Storage

2.6.1 Overview of coupling hydrogen production with CO_2 storage

The concepts of serpentinization and carbon mineralization have previously been viewed as mutually exclusive events, but the notion of a combinatory process of these two geological processes counts as enticingly rewarding if these processes could be optimized and scaled up in the right manner. In the carbon mineralization process, compressed carbon dioxide, technically, supercritical CO_2 from either point source or captured elsewhere is pumped through pipelines into rocks, or saline aquifers which allows for the evolution and precipitation of carbonate minerals. Though a series of rocks have been assessed, the possibility of utilizing various types of soils seems feasible based on kinetics [112], and even for manure and compost [113]. Safety is paramount in the process because once the fluid encounters the rocks, the dissolution and precipitation events cannot be fully predicted[114], though simulation studies and artificial intelligence methods are utilised to mitigate instances of leakages and possible seismic events [115]

It is surely refreshing that the same ultramafic rocks which have been examined for their potential to store CO_2 can also be used for producing hydrogen [8], [116]. This procedure entails recovering the water, infused with hydrogen, from nearby retrieval wells positioned around the injection area after injecting water directly into targeted reactive formations [8]. The natural occurrence of serpentinization and hydrogen production takes place at long-time scales since most natural serpentinization processes occur at lower temperatures thus the thermodynamics do not favour faster kinetics, but in the “artificial” process, the temperature and pressure, and even for what it is worth, the introduction of specific catalysts, though the

latter's effectiveness not extensively assessed can be tuned to reflect faster kinetic and reaction extents and high hydrogen generation events.

It goes without saying that, for the "artificially" generated temperatures which would drive these processes, high substantive energy inputs will be required. Also, the carbon mineralization process introduces hefty effects due to the precipitation of carbonate minerals, on the petrophysical characteristics of the rocks, both on their porosity and permeability and this would have a consequent effect on the generated hydrogen with time [117], but the rationale is just as simple as the effective synergistic use of geological resources in storing carbon dioxide and producing hydrogen, and the production of carbon-neutral hydrogen thus reducing anthropogenic emissions and minimising the over-reliance on fossil fuel.

Table 2.2 Laboratory Experiments on Coupled Process

Objective	Experimental Conditions	Reactant and Product Analysis	Reference
Assessing the twin process of carbonation and serpentinization in a serpentinite	The serpentinite cores, measuring approximately 3–4 cm in length and 5.6 mm in diameter, underwent a continuous injection process with a brine saturated with NaHCO3 for a duration of around 10 days at temperatures of 160°C and 280°C, respectively.	Serpentinite as reactant with precipitation of magnesite, calcites, and hematite	[117]
Coupled process of iron oxidation and CO2 sequestration on mine tailings	473 K/15 MPa, 523 K/30 MPa and 573 K/30 MPa conducted for 25 days	Mine tailings used as reactants with the precipitation of Fe-bearing magnesite	[118]
Using NAHCO3 in producing hydrogen and storing CO2	Lab experiment conducted at 300 °C for 72 hours	Olivine used as reactants with CO2 reduced to formic acid (HCOOH) or sequestrated in magnesite (MgCO3)	[119]

Objective	Experimental Conditions	Reactant and Product Analysis	Reference
Considering the effects of temperature on Olivine in NAHCO3 solutions	Reactions under temperature ranging from 225 - 300 °C for 72 hours	Olivine as reactants and CO2 was simultaneously stored as magnesite	[120]
Producing hydrogen by reacting water with steel slags	Reaction proceeded from 2- 57 days at 50 MPa for temperatures ranging from 473 to 673 K	Steel slag with variations in minerals of magnesite, larnite, calcite, aragonite, portlandite etc.	[121]
Assessing H2 generation and CO2 storage on reacting water with Olivine-Orthopyroxene	0.5 M NaHCO3 solution used at 300°C and 10 MPa with reaction proceeding for 120 hours	Olivine and orthopyroxene as reactants with varying precipitation of serpentine, magnesite, magnetite, and talc.	[122]
Evaluation of CO2 effect on H2 generation and minerals evolution	0.5 M NaHCO3 solution used at 300°C and 10 Mpa with reaction proceeding for 144 hours	CO2 underwent concurrent hydrogenation to form formic acid (HCOOH) using generated H2 and was simultaneously carbonated to produce magnesite.	[9]

Objective	Experimental Conditions	Reactant and Product Analysis	Reference
Evaluating the dissolution of olivine while considering hydrogen generation and CO2 storage in alkaline solutions	Reaction performed with NaHCO3 in high pH ranging from 8 - 11	Olivine as reactants with formation of chrysotile, magnesite, and negligible amounts of suppressed brucite	[123]
Assessing the effects of spinel in reaction kinetics of olivine in hydrogen generation and CO2 storage	0.5 M NaHCO3) solution under hydrothermal conditions (300°C and 10 MPa) for 72 hours	Mineral measurements indicated that an increased amount of aluminium, originating from the Mg-Al spinel, was assimilated into aluminium-rich serpentine through the substitution of iron, particularly in samples with higher Mg-Al spinel content.	[63]
Hydrogen generation as a result of Olivine and CO2 rich seawater	Reaction proceeded for 3000 hours at 300 °C, and pressure of 500 bars.	Olivine as reactants with the formation of Carbonate minerals, magnesite, and minor amount of dolomite	[124]

Objective	Experimental Conditions	Reactant and Product Analysis	Reference
Producing hydrogen and sequestering Co2 using mine tailings	Reactions were performed between temperature of 473 K and 573 K and partial pressure of CO2 between 15 MPa and 30 MPa	Mine tailings as reactants and precipitation of iron-rich magnesite	[125]
Evaluating the carbon distribution linked to the hydrothermal breakdown of siderite	Reactions proceeded for 2880 hours and a temperature range of 200–300 °C and at 50 MPa	Siderite as reactants with the precipitation of magnetite with carbon phases on its surface	[126]
Assessing the effecting of spinels (chromitite) on methane generation	300°C, 500 bars and proceeded for 1200 hours	Chromitite as reactants with formations of chlorite and Ferchromide	[127]
Hydrogen generation on synthetic komatite reaction with CO2-rich acidic NaCl fluid	Reaction proceeded for 3000 hours at 250 and 350 °C, and pressure of 500 bars.	Synthetic komatite as reactants, with the precipitation of komatiites carbonating to yield iron-rich dolomite (3–9 wt.% FeO) at 250 °C and calcite	[128]

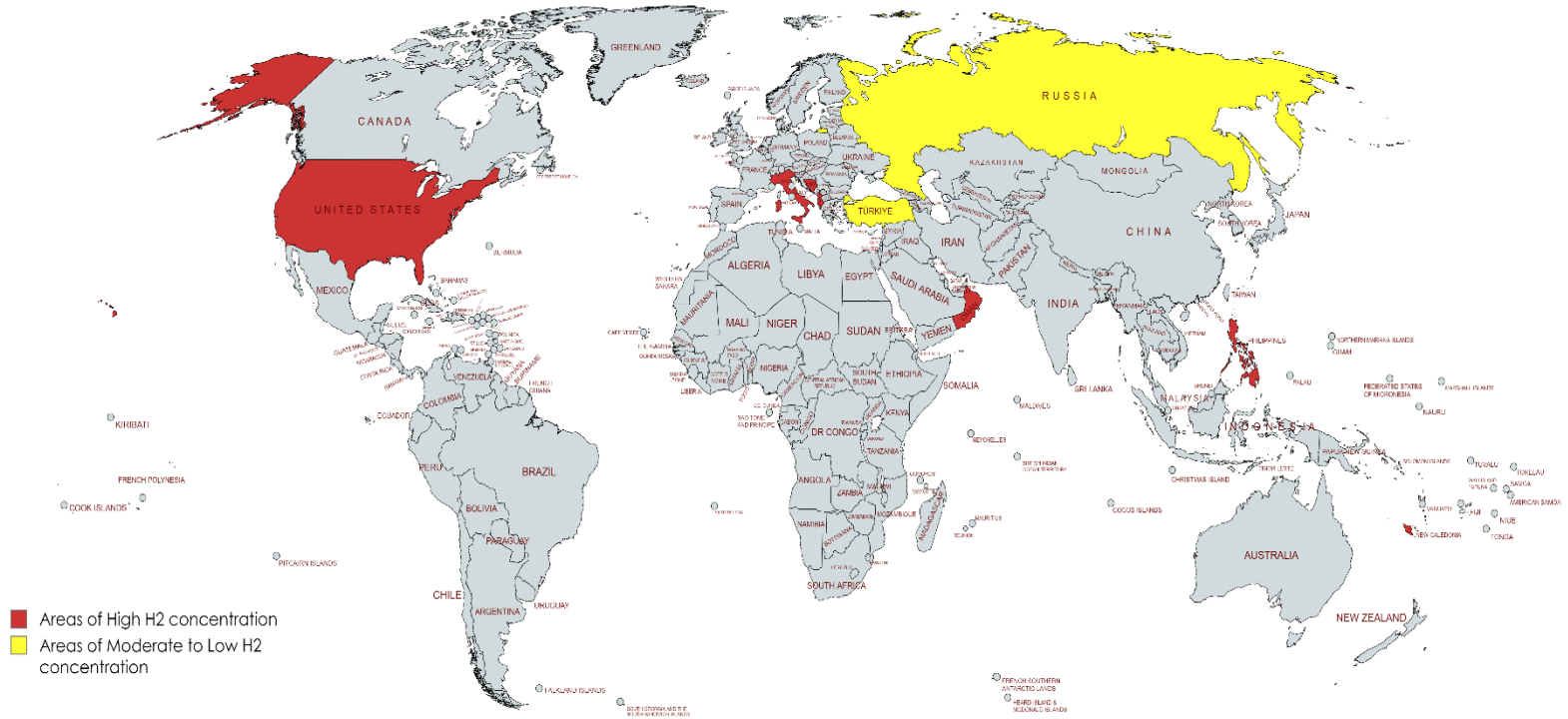

Figure 2.8 Map highlighting areas of serpentinization reactions around the world. Red areas depict areas of high hydrogen concentrations, and areas marked yellow depict moderate to low hydrogen concentrations.

2.7 Challenges Surrounding Serpentinization Reactions for H_2 Production

- **Slow kinetics**: Some natural hydrogen production processes, like serpentinization, can be slow, taking thousands to millions of years to produce significant amounts of hydrogen**.**
- **Environmental Impact**: Large-scale extraction of hydrogen from natural sources could have environmental consequences, including habitat destruction and groundwater contamination, coupled with induced seismicity.
- **Contaminant Issues**: Hydrogen produced through natural processes may be contaminated with impurities, and or bacterial activities requiring additional purification steps to meet quality standards for various applications.
- **Limited accessibility**: Hydrogen produced naturally may be trapped in inaccessible locations deep within the Earth's crust or mineral structures, making extraction difficult and costly.

2.8 Areas Needing Further Assessment

- In the coupled reaction process of serpentinization and carbon dioxide storage, engineers need to be informed of the petrophysical changes with time. Little is still known about how porosity and permeability change with time during these reactions, as such, Xray CT together with pore-scale modelling techniques need to be applied to assess these petrophysical changes.
- In serpentinization reactions, bacteria effects possibly hamper the amount and quality of hydrogen produced, thus the effects of bacteria on hydrogen produced during serpentinization reactions need assessment, especially at varying thermodynamic conditions.
- It has been highlighted that water plays a key role in hydrogen generation during serpentinization reactions, and temperature effects on reaction kinetics, but water-rock interactions in pores spaces in ultramafic rocks at the molecular level are still not understood. Methods such as molecular dynamic simulations can prove effective in providing such an understanding of the interaction in the pore spaces together with kinetics at the molecular level.
- In coupled reactions, the Fe-end member of olivine (fayalite) needs an assessment of its hydrogen and carbon dioxide storage abilities. Though most terrestrial mantle rocks are made of forsterites, iron-rich fayalite has proven effective in producing large

amounts of hydrogen, and its effectiveness in storing CO2 needs to be examined in a twin process.

- XRD and SEM have been used in determining the pre-experimental and post-experimental composition of samples, but they are time-consuming. Complimentary methods like Generative adversarial Neural Networks can be trained to produce synthetic images of these samples which can be used in Convolution neural Networks for mineral identification tasks.
- In the coupled reaction process of serpentinization reactions and CO_2 storage, pressure effects together with longer-term experiments especially on peridotites are sparse. Further assessment is needed to evaluate the effects of the thermodynamic variable on the processes.
- Various works have proven the effectiveness of spinels in serpentinization and CO_2 storage processes. It will be prudent to evaluate and compare the efficacy of various spinels/ catalysts on serpentinization and the coupled process of CO_2 storage and hydrogen production.
- Factors such as porosity, mineral composition, and water content can significantly affect radiation behaviour and its interaction with water within rocks. However, models used in explaining radiolytic reactions have mostly explained the process in the context of nuclear fuels, and the few that have studied the process at the water-solid interface neither validate the model on the radioactive rock-water interface nor adequately account for the specific properties of rocks that can influence radiation attenuation and radiolytic reactions.

REFERENCES

[1] S. Fudge and M. Peters, “Motivating carbon reduction in the UK: the role of local government as an agent of social change,” *Journal of Integrative Environmental Sciences*, vol. 6, no. 2, pp. 103–120, Jun. 2009, doi: 10.1080/19438150902732101.

[2] H. Liu, H. Lu, and H. Hu, “CO2 capture and mineral storage: State of the art and future challenges,” *Renewable and Sustainable Energy Reviews*, vol. 189. Elsevier Ltd, Jan. 01, 2024. doi: 10.1016/j.rser.2023.113908.

[3] A. I. Osman *et al.*, “Hydrogen production, storage, utilisation and environmental impacts: a review,” *Environmental Chemistry Letters*, vol. 20, no. 1. Springer Science and Business Media Deutschland GmbH, pp. 153–188, Feb. 01, 2022. doi: 10.1007/s10311-021-01322-8.

[4] K. Loiseau *et al.*, “Hydrogen generation and heterogeneity of the serpentinization process at all scales: Turon de Técouère lherzolite case study, Pyrenees (France),” *Geoenergy*, vol. 2, no. 1, Dec. 2024, doi: 10.1144/geoenergy2023-024.

[5] C. Olivares, J. Findlay, R. Kelly, S. Otto, M. Norman, and M. Cairns, “A new exploration tool in the search for native hydrogen and helium,” *Geological Society, London, Special Publications*, vol. 547, no. 1, Dec. 2024, doi: 10.1144/sp547-2023-49.

[6] M. Mahesh and P. B. Barker, “The MRI Helium Crisis: Past and Future,” *Journal of the American College of Radiology*, vol. 13, no. 12, pp. 1536–1537, Dec. 2016, doi: 10.1016/j.jacr.2016.07.038.

[7] O. Massarweh, M. Al-khuzaei, M. Al-Shafi, Y. Bicer, and A. S. Abushaikha, “Blue hydrogen production from natural gas reservoirs: A review of application and feasibility,” *Journal of CO2 Utilization*, vol. 70. Elsevier Ltd, Apr. 01, 2023. doi: 10.1016/j.jcou.2023.102438.

[8] F. Osselin, C. Soulaine, C. Fauguerolles, E. C. Gaucher, B. Scaillet, and M. Pichavant, “Orange hydrogen is the new green,” *Nat Geosci*, vol. 15, no. 10, pp. 765–769, Oct. 2022, doi: 10.1038/s41561-022-01043-9.

[9] J. Wang, K. Nakamura, N. Watanabe, A. Okamoto, and T. Komai, “Simultaneous H2 Production with Carbon Storage by Enhanced Olivine Weathering in Laboratory-scale: An Investigation of CO2 Effect,” Scitepress, May 2019, pp. 83–87. doi: 10.5220/0008186000830087.

[10] I. Renewable Energy Agency, *Making the breakthrough: Green hydrogen policies and technology costs*. 2021. [Online]. Available: www.irena.org

[11] T. Z. Ang, M. Salem, M. Kamarol, H. S. Das, M. A. Nazari, and N. Prabaharan, “A comprehensive study of renewable energy sources: Classifications, challenges and suggestions,” *Energy Strategy Reviews*, vol. 43. Elsevier Ltd, Sep. 01, 2022. doi: 10.1016/j.esr.2022.100939.

[12] O. Maiga, E. Deville, J. Laval, A. Prinzhofer, and A. B. Diallo, “Characterization of the spontaneously recharging natural hydrogen reservoirs of Bourakebougou in Mali,” *Sci Rep*, vol. 13, no. 1, Dec. 2023, doi: 10.1038/s41598-023-38977-y.

[13] A. Prinzhofer, C. S. Tahara Cissé, and A. B. Diallo, “Discovery of a large accumulation of natural hydrogen in Bourakebougou (Mali),” *Int J Hydrogen Energy*, vol. 43, no. 42, pp. 19315–19326, Oct. 2018, doi: 10.1016/j.ijhydene.2018.08.193.

[14] V. Zgonnik, “The occurrence and geoscience of natural hydrogen: A comprehensive review,” *Earth-Science Reviews*, vol. 203. Elsevier B.V., Apr. 01, 2020. doi: 10.1016/j.earscirev.2020.103140.

[15] Q. ning Tian, S. qing Yao, M. juan Shao, W. Zhang, and H. hua Wang, “Origin, discovery, exploration and development status and prospect of global natural hydrogen

under the background of ‘carbon neutrality,’” *China Geology*, vol. 5, no. 4. KeAi Communications Co., pp. 722–733, Oct. 01, 2022. doi: 10.31035/cg2022046.
[16] M. E. Dzaugis, A. J. Spivack, A. G. Dunlea, R. W. Murray, and S. D’Hondt, “Radiolytic hydrogen production in the subseafloor basaltic aquifer,” *Front Microbiol*, vol. 7, no. FEB, Feb. 2016, doi: 10.3389/fmicb.2016.00076.
[17] S. P. Gregory, M. J. Barnett, L. P. Field, and A. E. Milodowski, “Subsurface microbial hydrogen cycling: Natural occurrence and implications for industry,” *Microorganisms*, vol. 7, no. 2. MDPI AG, Feb. 01, 2019. doi: 10.3390/microorganisms7020053.
[18] N. Mahlstedt *et al.*, “Molecular hydrogen from organic sources in geological systems,” *J Nat Gas Sci Eng*, vol. 105, Sep. 2022, doi: 10.1016/j.jngse.2022.104704.
[19] F. Klein, W. Bach, N. Jöns, T. McCollom, B. Moskowitz, and T. Berquó, “Iron partitioning and hydrogen generation during serpentinization of abyssal peridotites from 15°N on the Mid-Atlantic Ridge,” *Geochim Cosmochim Acta*, vol. 73, no. 22, pp. 6868–6893, Nov. 2009, doi: 10.1016/j.gca.2009.08.021.
[20] H. M. Miller, L. E. Mayhew, E. T. Ellison, P. Kelemen, M. Kubo, and A. S. Templeton, “Low temperature hydrogen production during experimental hydration of partially-serpentinized dunite,” *Geochim Cosmochim Acta*, vol. 209, pp. 161–183, Jul. 2017, doi: 10.1016/j.gca.2017.04.022.
[21] T. M. McCollom, F. Klein, B. Moskowitz, T. S. Berquó, W. Bach, and A. S. Templeton, “Hydrogen generation and iron partitioning during experimental serpentinization of an olivine–pyroxene mixture,” *Geochim Cosmochim Acta*, vol. 282, pp. 55–75, Aug. 2020, doi: 10.1016/j.gca.2020.05.016.
[22] N. G. Holm, C. Oze, O. Mousis, J. H. Waite, and A. Guilbert-Lepoutre, “Serpentinization and the Formation of H2 and CH4 on Celestial Bodies (Planets, Moons, Comets),” *Astrobiology*, vol. 15, no. 7, pp. 587–600, Jul. 2015, doi: 10.1089/ast.2014.1188.
[23] L. Schwander, M. Brabender, N. Mrnjavac, J. L. E. Wimmer, M. Preiner, and W. F. Martin, “Serpentinization as the source of energy, electrons, organics, catalysts, nutrients and pH gradients for the origin of LUCA and life,” *Frontiers in Microbiology*, vol. 14. Frontiers Media SA, 2023. doi: 10.3389/fmicb.2023.1257597.
[24] T. M. McCollom and W. Bach, “Thermodynamic constraints on hydrogen generation during serpentinization of ultramafic rocks,” *Geochim Cosmochim Acta*, vol. 73, no. 3, pp. 856–875, Feb. 2009, doi: 10.1016/j.gca.2008.10.032.
[25] I. P. Hutchinson, O. Jackson, A. E. Stocks, A. C. Barnicoat, and S. R. Lawrence, “Greenstones as a source of hydrogen in cratonic sedimentary basins,” *Geological Society, London, Special Publications*, vol. 547, no. 1, Dec. 2024, doi: 10.1144/sp547-2023-39.
[26] Y. Dilek and H. Furnes, “Ophiolites and their origins,” *Elements*, vol. 10, no. 2, pp. 93–100, 2014, doi: 10.2113/gselements.10.2.93.
[27] M. Debure *et al.*, “Thermodynamic evidence of giant salt deposit formation by serpentinization: an alternative mechanism to solar evaporation,” *Sci Rep*, vol. 9, no. 1, Dec. 2019, doi: 10.1038/s41598-019-48138-9.
[28] L. Truche *et al.*, “A deep reservoir for hydrogen drives intense degassing in the Bulqizë ophiolite.” [Online]. Available: https://www.science.org
[29] G. Etiope, N. Samardžić, F. Grassa, H. Hrvatović, N. Miošić, and F. Skopljak, “Methane and hydrogen in hyperalkaline groundwaters of the serpentinized Dinaride ophiolite belt, Bosnia and Herzegovina,” *Applied Geochemistry*, vol. 84, pp. 286–296, Sep. 2017, doi: 10.1016/j.apgeochem.2017.07.006.
[30] C. Boulart, V. Chavagnac, C. Monnin, A. Delacour, G. Ceuleneer, and G. Hoareau, “Differences in gas venting from ultramafic-hosted warm springs: The example of oman

and voltri ophiolites," *Ofioliti*, vol. 38, no. 2, pp. 143–156, 2013, doi: 10.4454/ofioliti.v38i2.423.
[31] E. Deville and A. Prinzhofer, "The origin of N2-H2-CH4-rich natural gas seepages in ophiolitic context: A major and noble gases study of fluid seepages in New Caledonia," *Chem Geol*, vol. 440, pp. 139–147, Nov. 2016, doi: 10.1016/j.chemgeo.2016.06.011.
[32] V. Zgonnik, V. Beaumont, E. Deville, N. Larin, D. Pillot, and K. M. Farrell, "Evidence for natural molecular hydrogen seepage associated with Carolina bays (surficial, ovoid depressions on the Atlantic Coastal Plain, Province of the USA)," *Prog Earth Planet Sci*, vol. 2, no. 1, Dec. 2015, doi: 10.1186/s40645-015-0062-5.
[33] T. A. Abrajano, N. C. Sturchio, B. M. Kennedy, G. L. Lyon, K. Muehlenbachs, and J. K. Bohlke, "Geochemistry of reduced gas related to serpentinization of the Zambales ophiolite, Philippines," 1990.
[34] J. Guélard *et al.*, "Natural H2 in Kansas: Deep or shallow origin?," *Geochemistry, Geophysics, Geosystems*, vol. 18, no. 5, pp. 1841–1865, May 2017, doi: 10.1002/2016GC006544.
[35] V. Zgonnik, V. Beaumont, N. Larin, D. Pillot, and E. Deville, "Diffused flow of molecular hydrogen through the Western Hajar mountains, Northern Oman," *Arabian Journal of Geosciences*, vol. 12, no. 3, Feb. 2019, doi: 10.1007/s12517-019-4242-2.
[36] D. R. Meyer-Dombard *et al.*, "High pH microbial ecosystems in a newly discovered, ephemeral, serpentinizing fluid seep at Yanartaş (Chimera), Turkey," *Front Microbiol*, vol. 6, no. JAN, 2015, doi: 10.3389/fmicb.2014.00723.
[37] N. Larin, V. Zgonnik, S. Rodina, E. Deville, A. Prinzhofer, and V. N. Larin, "Natural Molecular Hydrogen Seepage Associated with Surficial, Rounded Depressions on the European Craton in Russia," *Natural Resources Research*, vol. 24, no. 3, pp. 369–383, Sep. 2015, doi: 10.1007/s11053-014-9257-5.
[38] P. L. Morrill *et al.*, "Geochemistry and geobiology of a present-day serpentinization site in California: The Cedars," *Geochim Cosmochim Acta*, vol. 109, pp. 222–240, May 2013, doi: 10.1016/j.gca.2013.01.043.
[39] C. Monnin *et al.*, "Fluid chemistry of the low temperature hyperalkaline hydrothermal system of Prony bay (New Caledonia)," *Biogeosciences*, vol. 11, no. 20, pp. 5687–5706, Oct. 2014, doi: 10.5194/bg-11-5687-2014.
[40] C. Vacquand *et al.*, "Reduced gas seepages in ophiolitic complexes: Evidences for multiple origins of the H2-CH4-N2 gas mixtures," *Geochim Cosmochim Acta*, vol. 223, pp. 437–461, Feb. 2018, doi: 10.1016/j.gca.2017.12.018.
[41] T. M. McCollom, F. Klein, and M. Ramba, "Hydrogen generation from serpentinization of iron-rich olivine on Mars, icy moons, and other planetary bodies," *Icarus*, vol. 372, Jan. 2022, doi: 10.1016/j.icarus.2021.114754.
[42] O. Maiga, E. Deville, J. Laval, A. Prinzhofer, and A. B. Diallo, "Characterization of the spontaneously recharging natural hydrogen reservoirs of Bourakebougou in Mali," *Sci Rep*, vol. 13, no. 1, Dec. 2023, doi: 10.1038/s41598-023-38977-y.
[43] R. Huang, M. Song, X. Ding, S. Zhu, W. Zhan, and W. Sun, "Influence of pyroxene and spinel on the kinetics of peridotite serpentinization," *J Geophys Res Solid Earth*, vol. 122, no. 9, pp. 7111–7126, Sep. 2017, doi: 10.1002/2017JB014231.
[44] T. M. McCollom *et al.*, "Temperature trends for reaction rates, hydrogen generation, and partitioning of iron during experimental serpentinization of olivine," *Geochim Cosmochim Acta*, vol. 181, pp. 175–200, May 2016, doi: 10.1016/j.gca.2016.03.002.
[45] R. Lafay, G. Montes-Hernandez, E. Janots, R. Chiriac, N. Findling, and F. Toche, "Mineral replacement rate of olivine by chrysotile and brucite under high alkaline conditions," *J Cryst Growth*, vol. 347, no. 1, 2012, doi: 10.1016/j.jcrysgro.2012.02.040ï.

[46] M. Andreani, I. Daniel, and M. Pollet-Villard, “Aluminum speeds up the hydrothermal alteration of olivine,” 2014.
[47] A. Neubeck, N. T. Duc, D. Bastviken, P. Crill, and N. G. Holm, “Formation of H2and CH4by weathering of olivine at temperatures between 30 and 70°C,” *Geochem Trans*, vol. 12, Jun. 2011, doi: 10.1186/1467-4866-12-6.
[48] R. Huang, W. Sun, M. Song, and X. Ding, “Influence of ph on molecular hydrogen (H2) generation and reaction rates during serpentinization of peridotite and olivine,” *Minerals*, vol. 9, no. 11, Nov. 2019, doi: 10.3390/min9110661.
[49] O. S. Pokrovsky and J. Schott, “PII S0016-7037(00)00434-8 Kinetics and mechanism of forsterite dissolution at 25°C and pH from 1 to 12,” 2000.
[50] T. M. McCollom, F. Klein, P. Solheid, and B. Moskowitz, “The effect of pH on rates of reaction and hydrogen generation during serpentinization,” *Philosophical Transactions of the Royal Society A: Mathematical, Physical and Engineering Sciences*, vol. 378, no. 2165, Feb. 2020, doi: 10.1098/rsta.2018.0428.
[51] C. Mével, “Serpentinisation des péridotites abysales aux dorsales océaniques,” *Comptes Rendus - Geoscience*, vol. 335, no. 10–11, pp. 825–852, 2003, doi: 10.1016/j.crte.2003.08.006.
[52] J. Noël, M. Godard, I. Martinez, M. Williams, M. Thierry, and F. Boudier, “Serpentinization in the Oman Ophiolite: oceanic to continental alteration processes in the Wadi Dima harzburgites (Wadi Tayin massif, Sultanate of Oman),” 2019.
[53] R. Huang, X. Shang, Y. Zhao, W. Sun, and X. Liu, “Effect of Fluid Salinity on Reaction Rate and Molecular Hydrogen (H2) Formation During Peridotite Serpentinization at 300°C,” *J Geophys Res Solid Earth*, vol. 128, no. 3, Mar. 2023, doi: 10.1029/2022JB025218.
[54] A. A. Olsen, E. M. Hausrath, and J. D. Rimstidt, “Forsterite dissolution rates in Mg-sulfate-rich Mars-analog brines and implications of the aqueous history of Mars,” *J Geophys Res Planets*, vol. 120, no. 3, pp. 388–400, Mar. 2015, doi: 10.1002/2014JE004664.
[55] H. M. Lamadrid *et al.*, “Effect of water activity on rates of serpentinization of olivine,” *Nat Commun*, vol. 8, Jul. 2017, doi: 10.1038/ncomms16107.
[56] F. Wang and D. E. Giammar, “Forsterite dissolution in saline water at elevated temperature and high CO2 pressure,” *Environ Sci Technol*, vol. 47, no. 1, pp. 168–173, Jan. 2013, doi: 10.1021/es301231n.
[57] B. Malvoisin, F. Brunet, J. Carlut, S. Rouméjon, and M. Cannat, “Serpentinization of oceanic peridotites: 2. Kinetics and processes of San Carlos olivine hydrothermal alteration,” *J Geophys Res Solid Earth*, vol. 117, no. 4, Apr. 2012, doi: 10.1029/2011JB008842.
[58] W. E. Seyfried, D. I. Foustoukos, and Q. Fu, “Redox evolution and mass transfer during serpentinization: An experimental and theoretical study at 200 °C, 500 bar with implications for ultramafic-hosted hydrothermal systems at Mid-Ocean Ridges,” *Geochim Cosmochim Acta*, vol. 71, no. 15, pp. 3872–3886, Aug. 2007, doi: 10.1016/j.gca.2007.05.015.
[59] V. Tsurkan, H. A. Krug von Nidda, J. Deisenhofer, P. Lunkenheimer, and A. Loidl, “On the complexity of spinels: Magnetic, electronic, and polar ground states,” *Physics Reports*, vol. 926. Elsevier B.V., pp. 1–86, Sep. 03, 2021. doi: 10.1016/j.physrep.2021.04.002.
[60] L. E. Mayhew, E. T. Ellison, T. M. McCollom, T. P. Trainor, and A. S. Templeton, “Hydrogen generation from low-temperature water-rock reactions,” *Nat Geosci*, vol. 6, no. 6, pp. 478–484, Jun. 2013, doi: 10.1038/ngeo1825.

[61] R. Huang, X. Ding, W. Sun, and X. Shang, “Contrasted effect of spinel and pyroxene on molecular hydrogen (H2) production during serpentinization of olivine,” *Minerals*, vol. 11, no. 8, Aug. 2021, doi: 10.3390/min11080794.
[62] R. Huang, W. Sun, X. Ding, Y. Zhao, and M. Song, “Effect of pressure on the kinetics of peridotite serpentinization,” *Phys Chem Miner*, vol. 47, no. 7, Jul. 2020, doi: 10.1007/s00269-020-01101-x.
[63] J. Wang, N. Watanabe, A. Okamoto, K. Nakamura, and T. Komai, “Characteristics of hydrogen production with carbon storage by CO2-rich hydrothermal alteration of olivine in the presence of Mg–Al spinel,” *Int J Hydrogen Energy*, vol. 45, no. 24, pp. 13163–13175, May 2020, doi: 10.1016/j.ijhydene.2020.03.032.
[64] D. L. Kohlstedt and S. J. Mackwcll, “Contributions to Mineralogy and Petrology High-temperature stability of San Carlos olivine,” 1987.
[65] A. Neubeck, N. T. Duc, D. Bastviken, P. Crill, and N. G. Holm, “Formation of H2and CH4by weathering of olivine at temperatures between 30 and 70°C,” *Geochem Trans*, vol. 12, Jun. 2011, doi: 10.1186/1467-4866-12-6.
[66] E. T. Ellison, A. S. Templeton, S. D. Zeigler, L. E. Mayhew, P. B. Kelemen, and J. M. Matter, “Low-Temperature Hydrogen Formation During Aqueous Alteration of Serpentinized Peridotite in the Samail Ophiolite,” *J Geophys Res Solid Earth*, vol. 126, no. 6, Jun. 2021, doi: 10.1029/2021JB021981.
[67] A. Boutier, A. Vitale Brovarone, I. Martinez, O. Sissmann, and S. Mana, “High-pressure serpentinization and abiotic methane formation in metaperidotite from the Appalachian subduction, northern Vermont,” *Lithos*, vol. 396–397, Sep. 2021, doi: 10.1016/j.lithos.2021.106190.
[68] Y. de M. Portella, R. V. Conceição, T. A. Siqueira, L. B. Gomes, and R. S. Iglesias, “Experimental evidence of pressure effects on spinel dissolution and peridotite serpentinization kinetics under shallow hydrothermal conditions,” *Geoscience Frontiers*, vol. 15, no. 2, Mar. 2024, doi: 10.1016/j.gsf.2023.101763.
[69] S. Schwartz *et al.*, “Pressure-temperature estimates of the lizardite/antigorite transition in high pressure serpentinites,” *Lithos*, vol. 178, pp. 197–210, Sep. 2013, doi: 10.1016/j.lithos.2012.11.023.
[70] U. Geymond, E. Ramanaidou, D. Lévy, A. Ouaya, and I. Moretti, “Can Weathering of Banded Iron Formations Generate Natural Hydrogen? Evidence from Australia, Brazil and South Africa,” *Minerals*, vol. 12, no. 2, Feb. 2022, doi: 10.3390/min12020163.
[71] V. Roche *et al.*, “A new continental hydrogen play in Damara Belt (Namibia),” *Sci Rep*, vol. 14, no. 1, Dec. 2024, doi: 10.1038/s41598-024-62538-6.
[72] “B9780128036891000080”.
[73] H. L. James and A. F. Trendall, “Banded Iron Formation: Distribution in Time and Paleoenvironmental Significance.”
[74] E. C. Fru *et al.*, “Sedimentary mechanisms of a modern banded iron formation on Milos Island, Greece,” *Solid Earth*, vol. 9, no. 3, pp. 573–598, May 2018, doi: 10.5194/se-9-573-2018.
[75] J. E. Johnson and P. H. Molnar, “Widespread and Persistent Deposition of Iron Formations for Two Billion Years,” *Geophys Res Lett*, vol. 46, no. 6, pp. 3327–3339, Mar. 2019, doi: 10.1029/2019GL081970.
[76] J. Yin, H. Li, and K. Xiao, “Origin of Banded Iron Formations: Links with Paleoclimate, Paleoenvironment, and Major Geological Processes,” *Minerals*, vol. 13, no. 4. MDPI, Apr. 01, 2023. doi: 10.3390/min13040547.
[77] R. T. Anderson, F. H. Chapelle, and D. R. Lovley, “Evidence Against Hydrogen-Based Microbial Ecosystems in Basalt Aquifers.” [Online]. Available: https://www.science.org

[78] T. O. Stevens and J. P. McKinley, “Abiotic controls on H2 production from Basalt - Water reactions and implications for aquifer biogeochemistry,” *Environ Sci Technol*, vol. 34, no. 5, pp. 826–831, 2000, doi: 10.1021/es990583g.
[79] “science.270.5235.450”.
[80] J. Telling *et al.*, “Rock comminution as a source of hydrogen for subglacial ecosystems,” *Nat Geosci*, vol. 8, no. 11, pp. 851–855, Oct. 2015, doi: 10.1038/ngeo2533.
[81] F. Delogu, “Hydrogen generation by mechanochemical reaction of quartz powders in water,” *Int J Hydrogen Energy*, vol. 36, no. 23, pp. 15145–15152, Nov. 2011, doi: 10.1016/j.ijhydene.2011.08.120.
[82] J. Li and I. M. Chou, “Hydrogen in silicate melt inclusions in quartz from granite detected with Raman spectroscopy,” *Journal of Raman Spectroscopy*, vol. 46, no. 10, pp. 983–986, Oct. 2015, doi: 10.1002/jrs.4644.
[83] J. Murray, A. Clément, B. Fritz, J. Schmittbuhl, V. Bordmann, and J. M. Fleury, “Abiotic hydrogen generation from biotite-rich granite: A case study of the Soultz-sous-Forêts geothermal site, France,” *Applied Geochemistry*, vol. 119, Aug. 2020, doi: 10.1016/j.apgeochem.2020.104631.
[84] S. Le Caër, “Water radiolysis: Influence of oxide surfaces on H2 production under ionizing radiation,” *Water (Switzerland)*, vol. 3, no. 1. MDPI AG, pp. 235–253, 2011. doi: 10.3390/w3010235.
[85] M. E. Dzaugis, A. J. Spivack, and S. D’Hondt, “A quantitative model of water radiolysis and chemical production rates near radionuclide-containing solids,” *Radiation Physics and Chemistry*, vol. 115, pp. 127–134, Jul. 2015, doi: 10.1016/j.radphyschem.2015.06.011.
[86] A. Bouquet, C. R. Glein, D. Wyrick, and J. H. Waite, “ Alternative Energy: Production of H 2 by Radiolysis of Water in the Rocky Cores of Icy Bodies ,” *Astrophys J Lett*, vol. 840, no. 1, p. L8, May 2017, doi: 10.3847/2041-8213/aa6d56.
[87] C. Sartorio *et al.*, “Preliminary Assessment of Radiolysis for the Cooling Water System in the Rotating Target of SORGENTINA-RF,” *Environments - MDPI*, vol. 9, no. 8, Aug. 2022, doi: 10.3390/environments9080106.
[88] I. G. Draganić, “Radiolysis of water: A look at its origin and occurrence in the nature,” *Radiation Physics and Chemistry*, vol. 72, no. 2–3, pp. 181–186, 2005, doi: 10.1016/j.radphyschem.2004.09.012.
[89] J. DeWitt, S. McMahon, and J. Parnell, “The Effect of Grain Size on Porewater Radiolysis,” *Earth and Space Science*, vol. 9, no. 6, Jun. 2022, doi: 10.1029/2021EA002024.
[90] F. Nielsen and M. Jonsson, “Geometrical α- and β-dose distributions and production rates of radiolysis products in water in contact with spent nuclear fuel,” *Journal of Nuclear Materials*, vol. 359, no. 1–2, pp. 1–7, Dec. 2006, doi: 10.1016/j.jnucmat.2006.08.001.
[91] R. Karolytė *et al.*, “The role of porosity in H2/He production ratios in fracture fluids from the Witwatersrand Basin, South Africa,” *Chem Geol*, vol. 595, Apr. 2022, doi: 10.1016/j.chemgeo.2022.120788.
[92] M. Dzaugis, A. J. Spivack, and S. D’Hondt, “Radiolytic H2 production in martian environments,” *Astrobiology*, vol. 18, no. 9, pp. 1137–1146, Sep. 2018, doi: 10.1089/ast.2017.1654.
[93] S. Mcmahon, J. Parnell, and N. J. F. Blamey, “Evidence for seismogenic hydrogen gas, a potential microbial energy source on Earth and Mars.”
[94] L. Frances, M. Grivet, J. P. Renault, J. E. Groetz, and D. Ducret, “Hydrogen radiolytic release from zeolite 4A/water systems under γ irradiations,” *Radiation Physics and Chemistry*, vol. 110, pp. 6–11, May 2015, doi: 10.1016/j.radphyschem.2015.01.008.

[95] R. Mosser-Ruck *et al.*, “Serpentinization and H2 production during an iron-clay interaction experiment at 90C under low CO2 pressure,” *Appl Clay Sci*, vol. 191, Jun. 2020, doi: 10.1016/j.clay.2020.105609.
[96] C. Marcaillou, M. Muñoz, O. Vidal, T. Parra, and M. Harfouche, “Mineralogical evidence for H2 degassing during serpentinization at 300°C/300bar,” *Earth Planet Sci Lett*, vol. 303, no. 3–4, pp. 281–290, Mar. 2011, doi: 10.1016/j.epsl.2011.01.006.
[97] R. J. P. Williams, “A comparison of types of catalyst: The quality of metallo-enzymes,” *Journal of Inorganic Biochemistry*, vol. 102, no. 1. pp. 1–25, Jan. 2008. doi: 10.1016/j.jinorgbio.2007.08.012.
[98] M. Preiner, J. C. Xavier, A. Do Nascimento Vieira, K. Kleinermanns, J. F. Allen, and W. F. Martin, “Catalysts, autocatalysis and the origin of metabolism,” *Interface Focus*, vol. 9, no. 6. Royal Society Publishing, Dec. 06, 2019. doi: 10.1098/rsfs.2019.0072.
[99] K. Yan *et al.*, “Microwave-enhanced methane cracking for clean hydrogen production in shale rocks,” *Int J Hydrogen Energy*, vol. 48, no. 41, pp. 15421–15432, May 2023, doi: 10.1016/j.ijhydene.2023.01.052.
[100] Q. Yuan, X. Jie, and B. Ren, “Hydrogen generation in crushed rocks saturated by crude oil and water using microwave heating,” *Int J Hydrogen Energy*, vol. 47, no. 48, pp. 20793–20802, Jun. 2022, doi: 10.1016/j.ijhydene.2022.04.217.
[101] Q. Yuan, X. Jie, and B. Ren, “Hydrogen generation in crushed rocks saturated by crude oil and water using microwave heating,” *Int J Hydrogen Energy*, vol. 47, no. 48, pp. 20793–20802, Jun. 2022, doi: 10.1016/j.ijhydene.2022.04.217.
[102] X. Jie *et al.*, “On the performance optimisation of Fe catalysts in the microwave - assisted H2 production by the dehydrogenation of hexadecane,” *Catal Today*, vol. 317, pp. 29–35, Nov. 2018, doi: 10.1016/j.cattod.2018.03.036.
[103] F. M. Alptekin and M. S. Celiktas, “Review on Catalytic Biomass Gasification for Hydrogen Production as a Sustainable Energy Form and Social, Technological, Economic, Environmental, and Political Analysis of Catalysts,” *ACS Omega*, vol. 7, no. 29. American Chemical Society, pp. 24918–24941, Jul. 26, 2022. doi: 10.1021/acsomega.2c01538.
[104] G. Etiope and G. Martinelli, “Migration of carrier and trace gases in the geosphere: an overview,” 2002.
[105] G. Etiope and M. J. Whiticar, “Abiotic methane in continental ultramafic rock systems: Towards a genetic model,” *Applied Geochemistry*, vol. 102. Elsevier Ltd, pp. 139–152, Mar. 01, 2019. doi: 10.1016/j.apgeochem.2019.01.012.
[106] Z. Su *et al.*, “Research progress of ruthenium-based catalysts for hydrogen production from ammonia decomposition,” *International Journal of Hydrogen Energy*, vol. 51. Elsevier Ltd, pp. 1019–1043, Jan. 02, 2024. doi: 10.1016/j.ijhydene.2023.09.107.
[107] K. Steinthorsdottir, G. M. Dipple, J. A. Cutts, C. C. Turvey, D. Milidragovic, and S. M. Peacock, “Formation and Preservation of Brucite and Awaruite in Serpentinized and Tectonized Mantle in Central British Columbia: Implications for Carbon Mineralization and Nickel Mining,” *Journal of Petrology*, vol. 63, no. 11, Nov. 2022, doi: 10.1093/petrology/egac100.
[108] S. Seiler, P. Bradshaw, and B. Klein, “Awaruite, a new large nickel resource: Activation by ammonium sulfate and thiosulfate for flotation,” *Chemical Engineering Journal Advances*, vol. 13, Mar. 2023, doi: 10.1016/j.ceja.2022.100441.
[109] K. A. Evans, B. R. Frost, S. M. Reddy, and T. C. Brown, “Causes, effects, and implications of the relationships amongst fluids, serpentinisation, and alloys,” *Lithos*, vol. 446–447, Jun. 2023, doi: 10.1016/j.lithos.2023.107132.

[110] J. A. LaVerne and L. Tandon, “H2 production in the radiolysis of water on CeO2 and ZrO2,” *Journal of Physical Chemistry B*, vol. 106, no. 2, pp. 380–386, Jan. 2002, doi: 10.1021/jp013098s.
[111] J. F. Sauvage *et al.*, “The contribution of water radiolysis to marine sedimentary life,” *Nat Commun*, vol. 12, no. 1, Dec. 2021, doi: 10.1038/s41467-021-21218-z.
[112] R. Riffaldi, A. Saviozzi, and R. Levi-Minzi, “Carbon mineralization kinetics as influenced by soil properties,” Springer-Verlag, 1996.
[113] T. K. Hartz, J. P. Mitchell, and C. Giannini, “Nitrogen and Carbon Mineralization Dynamics of Manures and Composts,” 2000.
[114] J. M. Matter *et al.*, “Rapid carbon mineralization for permanent disposal of anthropogenic carbon dioxide emissions,” *Science (1979)*, vol. 352, no. 6291, pp. 1312–1314, Jun. 2016, doi: 10.1126/science.aad8132.
[115] P. Staša, K. Chovancová, V. Kebo, J. Chovanec, and O. Kodym, “Research of CO2 Storage Possibilities to the Underground,” *Procedia Earth and Planetary Science*, vol. 6, pp. 14–23, 2013, doi: 10.1016/j.proeps.2013.01.002.
[116] P. B. Kelemen *et al.*, “In situ carbon mineralization in ultramafic rocks: Natural processes and possible engineered methods,” in *Energy Procedia*, Elsevier Ltd, 2018, pp. 92–102. doi: 10.1016/j.egypro.2018.07.013.
[117] F. Osselin, M. Pichavant, R. Champallier, M. Ulrich, and H. Raimbourg, “Reactive transport experiments of coupled carbonation and serpentinization in a natural serpentinite. Implication for hydrogen production and carbon geological storage,” *Geochim Cosmochim Acta*, vol. 318, pp. 165–189, Feb. 2022, doi: 10.1016/j.gca.2021.11.039.
[118] K. Kularatne, O. Sissmann, E. Kohler, M. Chardin, S. Noirez, and I. Martinez, “Simultaneous ex-situ CO2 mineral sequestration and hydrogen production from olivine-bearing mine tailings,” *Applied Geochemistry*, vol. 95, pp. 195–205, Aug. 2018, doi: 10.1016/j.apgeochem.2018.05.020.
[119] J. Wang, N. Watanabe, A. Okamoto, K. Nakamura, and T. Komai, “Enhanced hydrogen production with carbon storage by olivine alteration in CO 2 -rich hydrothermal environments,” *Journal of CO2 Utilization*, vol. 30, pp. 205–213, Mar. 2019, doi: 10.1016/j.jcou.2019.02.008.
[120] J. Wang, N. Watanabe, A. Okamoto, K. Nakamura, and T. Komai, “Acceleration of hydrogen production during water-olivine-CO2 reactions via high-temperature-facilitated Fe(II) release,” *Int J Hydrogen Energy*, vol. 44, no. 23, pp. 11514–11524, May 2019, doi: 10.1016/j.ijhydene.2019.03.119.
[121] B. Malvoisin *et al.*, “High-purity hydrogen gas from the reaction between BOF steel slag and water in the 473-673 K range,” *Int J Hydrogen Energy*, vol. 38, no. 18, pp. 7382–7393, Jun. 2013, doi: 10.1016/j.ijhydene.2013.03.163.
[122] J. Wang, N. Watanabe, A. Okamoto, K. Nakamura, and T. Komai, “Pyroxene control of H2 production and carbon storage during water-peridotite-CO2 hydrothermal reactions,” *Int J Hydrogen Energy*, vol. 44, no. 49, pp. 26835–26847, Oct. 2019, doi: 10.1016/j.ijhydene.2019.08.161.
[123] J. Wang, K. Nakamura, N. Watanabe, A. Okamoto, and T. Komai, “NaHCO3-promoted olivine weathering with H2 generation and CO2 sequestration in alkaline hydrothermal system,” in *IOP Conference Series: Earth and Environmental Science*, Institute of Physics Publishing, May 2019. doi: 10.1088/1755-1315/257/1/012017.
[124] H. Ueda, Y. Sawaki, and S. Maruyama, “Reactions between olivine and CO2-rich seawater at 300 °C: Implications for H2 generation and CO2 sequestration on the early Earth,” *Geoscience Frontiers*, vol. 8, no. 2, pp. 387–396, Mar. 2017, doi: 10.1016/j.gsf.2016.10.002.

[125] T. L. Rapporteur, A. M. Rapporteur, M. C. Membre, V. -Brovarone, and A. Membre, "Carbon dioxide (CO 2) Valorization by Mineral Storage and Abiotic Hydrocarbons Generation Par Kanchana Kularatne Présentée et soutenue publiquement le 12 Juin 2018 Thèse de doctorat de Sciences de la Terre et de l'environnement Dirigée par Isabelle Martinez Devant un jury composé de."
[126] V. Milesi *et al.*, "Formation of CO2, H2 and condensed carbon from siderite dissolution in the 200-300°C range and at 50MPa," *Geochim Cosmochim Acta*, vol. 154, pp. 201–211, Apr. 2015, doi: 10.1016/j.gca.2015.01.015.
[127] H. Ueda, Y. Matsui, and Y. Sawaki, "Abiotic Methane Generation via CO2 Hydrogenation With Natural Chromitite Under Hydrothermal Conditions," *Geochemistry, Geophysics, Geosystems*, vol. 22, no. 4, Apr. 2021, doi: 10.1029/2020GC009533.
[128] H. Ueda, T. Shibuya, Y. Sawaki, M. Saitoh, K. Takai, and S. Maruyama, "Reactions between komatiite and CO2-rich seawater at 250 and 350 °C, 500 bars: implications for hydrogen generation in the Hadean seafloor hydrothermal system," *Prog Earth Planet Sci*, vol. 3, no. 1, Dec. 2016, doi: 10.1186/s40645-016-0111-8.
[129] F. Klein, N. G. Grozeva, and T. M. Mccollom, "Temperature Effects on Hydrogen Generation During Serpentinization," 2010.
[130] D. E. Allen and W. E. Seyfried, "Compositional controls on vent fluids from ultramafic-hosted hydrothermal systems at mid-ocean ridges: An experimental study at 4 00°C, 500 bars," *Geochim Cosmochim Acta*, vol. 67, no. 8, pp. 1531–1542, Apr. 2003, doi: 10.1016/S0016-7037(02)01173-0.
[131] T. M. McCollom, F. Klein, B. Moskowitz, T. S. Berquó, W. Bach, and A. S. Templeton, "Hydrogen generation and iron partitioning during experimental serpentinization of an olivine–pyroxene mixture," *Geochim Cosmochim Acta*, vol. 282, pp. 55–75, Aug. 2020, doi: 10.1016/j.gca.2020.05.016.
[132] L. S. Eti, "); A. Marton (Hungary, 1991-93); Associate Members," W. Engelwald, 1993.
[133] R. A. Shellie, "Gas Chromatography," in *Encyclopedia of Forensic Sciences: Second Edition*, Elsevier Inc., 2013, pp. 579–585. doi: 10.1016/B978-0-12-382165-2.00245-2.
[134] "Industrial Dyes: Chemistry, Properties, Applications Edited by Klaus Hunger (Kelkheim, Germany). Wiley-VCH: Weinheim. 2003. xxiv + 600 pp. $185.00. ISBN 3-527-30426-6.," *J Am Chem Soc*, vol. 125, no. 33, pp. 10144–10144, Aug. 2003, doi: 10.1021/ja0335418.
[135] C. M. Hussain and R. Keçili, "Separation techniques for environmental analysis," in *Modern Environmental Analysis Techniques for Pollutants*, Elsevier, 2020, pp. 163–198. doi: 10.1016/b978-0-12-816934-6.00007-2.
[136] "ICP- MAGU Labs".
[137] R. E. S. Froes, W. Borges Neto, R. L. P. Naveira, N. C. Silva, C. C. Nascentes, and J. B. B. da Silva, "Exploratory analysis and inductively coupled plasma optical emission spectrometry (ICP OES) applied in the determination of metals in soft drinks," *Microchemical Journal*, vol. 92, no. 1, pp. 68–72, May 2009, doi: 10.1016/j.microc.2008.12.008.
[138] R. Paranthaman, J. A. Moses, and C. Anandharamakrishnan, "Powder X-ray diffraction conditions for screening curcumin in turmeric powder," *Journal of Food Measurement and Characterization*, vol. 16, no. 2, pp. 1105–1113, Apr. 2022, doi: 10.1007/s11694-021-01225-w.
[139] A. Ali, Y. W. Chiang, and R. M. Santos, "X-Ray Diffraction Techniques for Mineral Characterization: A Review for Engineers of the Fundamentals, Applications, and Research Directions," *Minerals*, vol. 12, no. 2, Feb. 2022, doi: 10.3390/min12020205.
[140] "ryland-1958-x-ray-diffraction".

[141] S. Agatonovic-Kustrin and R. Beresford, “Basic concepts of artificial neural network (ANN) modeling and its application in pharmaceutical research,” 2000. [Online]. Available: www.elsevier.com/locate/jpba
[142] L. Yitian and R. R. Gu, “Modeling flow and sediment transport in a river system using an artificial neural network,” *Environ Manage*, vol. 31, no. 1, pp. 122–134, Jan. 2003, doi: 10.1007/s00267-002-2862-9.
[143] D. P. Kingma and J. Ba, “Adam: A Method for Stochastic Optimization,” Dec. 2014, [Online]. Available: http://arxiv.org/abs/1412.6980
[144] G.-B. Huang, Q.-Y. Zhu, and C.-K. Siew, “Extreme Learning Machine: A New Learning Scheme of Feedforward Neural Networks.”
[145] A. Jaiswal, S. Roy, G. Srinivasan, and K. Roy, “Proposal for a Leaky-Integrate-Fire Spiking Neuron based on Magneto-Electric Switching of Ferro-magnets,” Sep. 2016, doi: 10.1109/TED.2017.2671353.
[146] J. Wang, S. Lu, S. H. Wang, and Y. D. Zhang, “A review on extreme learning machine,” *Multimed Tools Appl*, vol. 81, no. 29, pp. 41611–41660, Dec. 2022, doi: 10.1007/s11042-021-11007-7.
[147] G. Goos *et al.*, “LNCS 3973 - Advances in Neural Networks - ISNN 2006,” 2006.
[148] X. C. Yang, X. R. Yan, and C. F. Song, “Pressure Prediction of Coal Slurry Transportation Pipeline Based on Particle Swarm Optimization Kernel Function Extreme Learning Machine,” *Math Probl Eng*, vol. 2015, 2015, doi: 10.1155/2015/542182.